

South Dakota State University

Open PRAIRIE: Open Public Research Access Institutional Repository and Information Exchange

Electronic Theses and Dissertations

2018

Development of Material for 3D Printed Habitats with Extraterrestrial Applications

Taylor Wait

South Dakota State University

Follow this and additional works at: <https://openprairie.sdstate.edu/etd>



Part of the [Materials Science and Engineering Commons](#), and the [Mechanical Engineering Commons](#)

Recommended Citation

Wait, Taylor, "Development of Material for 3D Printed Habitats with Extraterrestrial Applications" (2018). *Electronic Theses and Dissertations*. 2675. <https://openprairie.sdstate.edu/etd/2675>

This Thesis - Open Access is brought to you for free and open access by Open PRAIRIE: Open Public Research Access Institutional Repository and Information Exchange. It has been accepted for inclusion in Electronic Theses and Dissertations by an authorized administrator of Open PRAIRIE: Open Public Research Access Institutional Repository and Information Exchange. For more information, please contact michael.biondo@sdstate.edu.

DEVELOPMENT OF MATERIAL FOR 3D PRINTED HABITATS WITH
EXTRAPLANETARY APPLICATIONS

BY
TAYLOR WAIT

A thesis submitted in partial fulfillment of the requirements for the

Master of Science

Major in Mechanical Engineering

South Dakota State University

2018

DEVELOPMENT OF MATERIAL FOR 3D PRINTED HABITATS WITH
EXTRAPLANETARY APPLICATIONS

Taylor Wait

This thesis is approved as a creditable and independent investigation by a candidate for the Master of Science in Mechanical Engineering degree and is acceptable for meeting the thesis requirements for this degree. Acceptance of this does not imply that the conclusions reached by the candidate are necessarily the conclusions of the major department

Todd Letcher, Ph.D.

Thesis Advisor

Date

Kurt Basset, Ph.D.

Head, Department of Mechanical Engineering Date

Dean, Graduate School

Date

ACKNOWLEDGEMENTS

First off, I would like to thank Dr. Todd Letcher for being an excellent advisor, not only to me but the rest of the students doing research with him. He constantly challenges and encourages us to learn and do more, and to consider as many options as possible when we run in to trouble. His patience and dedication to his students is beyond compare. From late nights reviewing papers and homework, to the endless stream of students waiting outside of his office for help, he makes himself as available as possible, sometimes even more than should be humanly possible. In my opinion he is the perfect example of what a professor should be for students. Constantly challenging and pushing students to learn more, innovate, and inspiring them to even want to attempt something new in the first place.

Secondly, I would like to thank the METLAB and Dr. Fereidoon Delfanian who, through funding from the AMPTEC project, provided me with a research assistant position to help my work through graduate school. Without this position, grad school would never have been an option and I will be forever grateful for the opportunity and experience of working in the METLAB. I learned more about material properties and testing than I ever thought possible and got to use plenty of specialized equipment not normally available to students at any university. It was certainly a unique and extraordinary experience not offered to many.

I also want to thank the SDSU ARC team for volunteering to participate in the 3DPH Challenge. Not only is this an exciting opportunity for everyone on the team, but for the school to compete and be recognized internationally. The dedication and excitement from all the team members to participate and spend long hours designing,

research, and building cannot go without mention and I wish the team luck in the future of the competition.

Of course, I must thank my family, both immediate and my future in-laws. Their constant encouragement and questions have kept me motivated. Despite repeated jokes and comments of them not knowing what I'm talking about, they have kept me going and learning. Their questions kept me constantly thinking about the research and helped me to better understand my motivations, and my results.

Lastly, I must thank my fiancé, who by the time of publishing will be my wife. There is no way I could have ever completed my master's degree without your constant love, support, and reminders to go write my thesis. You have made my graduate school years the happiest of my life, and I cannot wait for the many happy years to come.

TABLE OF CONTENTS

LIST OF TABLES	vi
LIST OF FIGURES	vii
ABSTRACT.....	ix
CHAPTER 1: INTRODUCTION	1
CHAPTER 2: LITERATURE REVIEW	4
CHAPTER 3: METHOD AND APPROACH	11
3.1 Test Printer Design	11
3.2 Material Selection	14
3.3 3D Printed Habitat Challenge Printer	16
3.4 Molded Sample Test Plan	24
3.5 Flexural Testing	25
3.6 Compression Testing	27
3.7 Printed Sample Quality Testing	28
3.8 Printed Sample Strength Testing.....	30
CHAPTER 4: RESULTS.....	32
4.1 Digital Radiography Inspection of Molded Samples	32
4.2 Flexural Testing Results	36
4.3 Compressive Testing Results	42
4.4 3D Printed Habitat Challenge Printer	49
4.5 Qualitative Print Tests.....	58
4.6 Printed Sample Strength Testing.....	61
CHAPTER 5: CONCLUSIONS	71
REFERENCES	75

LIST OF TABLES

Table 1. Average Flexural Strength Values of Pure HDPE, CS, & FS Mixtures	42
Table 2. Average Compressive Strength Values of Pure HDPE, CS, & FS Mixtures.....	48
Table 3. Flexural Strength Values for All Tested Samples.....	65
Table 4. Compressive Strength Values for All Tested Samples	66
Table 5. Densities of All Mixture Types.....	67

LIST OF FIGURES

Figure 1. Test Printer Controls.....	12
Figure 2. Test Printer Front View	13
Figure 3. Test Printer Build Area.....	13
Figure 4. Printed Sulfur Sample.....	14
Figure 5. NASA Challenge Material Score Sheet.....	15
Figure 6. Extrusion System Model	18
Figure 7. Superstructure Model	20
Figure 8. Y-Axis Cart System Model	20
Figure 9. Superstructure Mounted on X-Axis Rail	21
Figure 10. X-Axis Rail Design	22
Figure 11. Print Head Structure	23
Figure 12. Full Printer Assembly	23
Figure 13. Melted Flex Samples in Molds	24
Figure 14. Melted Compression Samples in Molds	25
Figure 15. Flexural Test Setup.....	26
Figure 16. Compression Sample in Test Fixture.....	28
Figure 17. Test Printing Setup	29
Figure 18. Printing Tests in Progress.....	30
Figure 19. Flex Samples Cut from Printed Block.....	31
Figure 20. Radiograph of Pure HDPE Flex Samples (Left to Right 1,2,3).....	33
Figure 21. Radiograph of Pure HDPE Compression Samples (Left to Right 1,2,3).....	34
Figure 22. Radiograph Side View of 30% HDPE/CS Flex Specimens (Left to Right, 1-6).....	34
Figure 23. Radiograph of 30% HDPE/CS Compression Samples (Left to Right, 3-5)	35
Figure 24. Radiograph Comparison of (Left to Right) 20, 30, 40, and 50% HDPE/CS Mixtures.....	35
Figure 25. Flexural Failure of 50% HDPE/FS Specimen	36
Figure 26. (Left) Stress Strain Curve for 50% HDPE/FS Flex Specimen (Right) Stress-Strain with Modulus of Flexure Fit Line	37
Figure 27. Graph of Flexural Strength vs. Percent Plastic.....	39
Figure 28. Graph of Average Modulus of Flexure vs. Plastic Percentage	40
Figure 29. 20%HDPE/ FS Compression Specimen After Failure	43
Figure 30. 50%HDPE/ FS Compression Sample with Stress Crack and Mushrooming	43
Figure 31. (Left) Stress Strain Curve for 50% HDPE/FS Compression Specimen (Right) Stress-Strain with Modulus of Elasticity Fit Line.....	44
Figure 32. Compressive Yield Strength vs. Plastic Percentage	46
Figure 33. Modulus of Elasticity vs Percent Plastic for Compression Samples	48
Figure 34. X-Axis Rail Jig Assembly	50
Figure 35. Tower Build in Progress.....	50
Figure 36. Completed Printer.....	51
Figure 37. V Caster Track.....	52
Figure 38. X-Axis Motor and Rack	52
Figure 39. Y-Axis End View	53
Figure 40. Y-Axis Print Head Opening	54
Figure 41. Full View of Print Head	54
Figure 42. Z-Axis Motion System	55
Figure 43. Lead Screw and Linear Rod Mounting.....	56

Figure 44. Extruder Motor System	57
Figure 45. Extruder Heater Bands and Thermocouples	57
Figure 46. Final Results of First Test Print	59
Figure 47. Second Test Print Line Overlap.....	59
Figure 48. Print Five in Progress	60
Figure 49. Test Print Six in Process	61
Figure 50. Comparison of Printed (left) and Molded (right) Flex Samples of 30% HDPE/FS	62
Figure 51. Printed Flexural Sample in Test Fixture	63
Figure 52. Printed Compression Samples	64
Figure 53. Printed Compression Sample After Failure.....	64
Figure 54. Radiograph of 30% HDPE/FS Printed Sample (left), 20% Molded Sample (middle), and 30% Molded Samples (right)	68
Figure 55. Color Corrected Radiograph of 30% HDPE/FS Printed Sample (left), 20% Molded Sample (middle), and 30% Molded Samples (right).....	69

ABSTRACT

DEVELOPMENT OF MATERIAL FOR 3D PRINTED HABITATS WITH
EXTRAPLANETARY APPLICATIONS

TAYLOR WAIT

2018

3D printing, also called Additive Manufacturing, has increasingly become a focus for research because of the potential to replace complicated assemblies or complex parts with a single printed item. The space industry is very interesting in studying 3d printing with parts being tested and used on rockets, a 3D printer being installed at the International Space Station and is being developed for use in manned exploration of extraplanetary bodies to build habitats. To encourage teams from around the world to develop technologies and materials for autonomous habitat construction using minimal Earth exports, NASA created the 3D Printed Habitat Challenge. NASA is looking for creative and innovative materials and ideas from around the world to aid in reaching their own mission and research goals. To compete in the 3D Printed Habitat Challenge, a thermoplastic concrete was developed that can be 3D printed and used in the future exploration of the solar system. Using HDPE as a binder, the plastic was combined in various weight ratios with sand aggregates to find flexural and compressive strengths. Samples were created by molding mixtures, and later 3D printing with the optimum mixture. The optimum molded mixture was determined to be a 30%wt. HDPE, 70% wt. fine sand aggregate mix, which yielded a flexural yield stress of 14.03 ± 1.59 MPa, and a compressive yield stress of 15.27 ± 0.86 MPa. This mixture was then printed on the large

3D printer and saw increases in flexural and compressive yield strengths to 16.55 ± 0.32 MPa and 21.61 ± 0.04 MPa, respectively. This increase in strength has largely been attributed to the mixing and heating process that occurs organically via the extrusion process. This implies that mixing and heating in the extruder of a lower plastic content mixture could produce better results, with less plastic material. This is a major benefit when plastics are need for construction and must be exported to other planetary bodies.

CHAPTER 1: INTRODUCTION

In the last few years there has been a revival of sorts for space exploration. With the recent success of the Falcon Heavy by SpaceX [1], and the continued development of the Space Launch System (SLS) by NASA [2], manned exploration of the Moon and Mars is not only a possibility, but an inevitability. SpaceX CEO Elon Musk announced ambitious plans for their BFR rocket system to provide not only payload options for space agencies and satellites, but short flights around Earth, and relatively inexpensive trips to the Moon and Mars. Part of SpaceX's goal is to decrease the cost of rocket launches significantly, to make space travel more affordable to citizens who wish to explore our solar system [3].

Additive Manufacturing (AM), or 3D printing, has also been utilized for its rapid prototyping and cost effectiveness to improve a variety of industries, including rocketry. NASA tested a 3D printed pogo accumulator, used as a shock absorber, and cut costs by 35% and production time by 80% [4]. SpaceX also used a 3D printed Main Oxidizer Valve (MOV) in a Merlin engine on a January 6, 2014 rocket launch. The MOV was printed in two days, compared to a typical production cycle of months. SpaceX also successfully tested a printed Engine Chamber for their SuperDraco engines in late 2013 [5]. These tests are an unofficial milestone for 3D printing in many ways. Nearly every part on a rocket needs to work perfectly to prevent disaster. The testing and proving of viability for 3D printed parts in a critical role demonstrates the future potential for use of 3D printers and parts for missions.

NASA is also interested in 3D printing for use in habitat construction for manned missions to other planets and moons. The NASA 3D Printed Habitat Challenge (3DPH) was created and opened to the public world-wide to compete for prize money. The multi-phase challenge, currently in Phase 3, requires teams to design a habitat, as well as develop a material and system that can work autonomously using minimal imported material to build a habitat for future extraplanetary explorers to live [6]. The competition shows not only the potential uses, but likely necessity, of large scale 3D printing to enable manned exploration, and perhaps future colonization, of the solar system. The printing system also has the potential to be adapted for use on Earth as well for low-cost housing for poor or developing nations, or as potential disaster relief housing.

Increased attention to the potential of Additive Manufacturing (AM) has led to breakthroughs in machine designs, accuracy and potential uses. Of interest is the large-scale application of AM techniques to construction. Successful implementation could result in faster construction times, less waste material, and the optimization of designs to support structural loads. Another prime interest is the possibility of using AM on extraplanetary bodies to build structures using locally available materials. This would mean cost savings on launching building materials and fully built structures, as well as increased safety for manned missions. In the event of structural damage, a building could be repaired or replaced with local materials rather than risking lives or forcing a mission to end prematurely.

Large scale concrete printers have already been developed, but are limited to predefined work zones, and limited structural potential. They also require the use of water-based cement, which is not a feasible material on most extraplanetary bodies. At a

minimum, it would take more time and resources to gather the water required for construction. A preferred option would be to use locally sourced aggregates, along with recycled or waste thermoplastic as a binding agent. This would mean structures can be repaired or replaced with any locally available aggregates, with minimal processing. Using the extra plastics from launch-phase packaging and broken or unused parts would eliminate the need to bring extra construction materials to a location saving money on transport costs and those materials themselves.

Proving the viability of this process could also have a large impact on the environment of Earth as well. With increased consumer consumption of plastics and the growing demand for recycling options, a thermoplastic concrete could be used to remove damaging waste plastic from the environment and put it to a more productive use. Potential uses included sidewalks, parking lots, low traffic roads, or landscaping architecture. Implementing this composite material with an AM process could also provide fast emergency housing for disaster zones, and affordable low-income housing for impoverished areas. Use of a thermoplastic as a cement substitute would also mean easier, faster repairs on damaged structures. Thermoplastics can be reheated and formed into a new shape, or resealed, saving on repair time, costs, and reducing material waste.

CHAPTER 2: LITERATURE REVIEW

Large-scale 3D printing is an under-researched application, mostly due to the size and complexity of such a system. Some advanced machines have been built that can print a variety of materials, mostly related to water-based concrete. However, several other avenues for unique materials for use in extra-planetary based construction have also been explored.

Automation in fabrication of products has grown significantly in almost all areas, but growth in the construction industry has been slow due to complexity of buildings, making automation unsuitable at the current level of technology. There are also limitations on the material types that are suitable for automation. Dr. Behrokh Khoshnevis of the University of Southern California started development of a system – called Contour Crafting (CC) in 1998 [7]. The initial design used a specialized trowel head to smooth surfaces of a wide variety of printed materials, and create a variety of shapes and contours, which saves time for printing, and post fabrication work. As the printer extrudes material, the trowel would the shape and smooth out the top and outside face of the print. The machine also creates larger hatches to form the main body of the part, and the internal volumes are filled like molds. Khoshnevis also outlines other possibilities for the system to be able to extruder multiple materials in one print by having multiple lines to the extruder head that can be switched on/off during printing. There are some flaws, however, such as the size of parts that can be fabrication due to nozzle and trowel size, as well as the machine and software complexity needed to be able to control and move a trowel head about the object.

In further development, Khoshnevis outlined other potentials for the machine. The flexibility of the system would allow exotic, yet functional geometries to be constructed that are difficult to build with conventional construction practices. With further development, the system could also embed conduit, electrical and communication wiring, plumbing, even floor and wall tiling. The computer control of the CC system could also allow for the control of laying smart materials that can be precisely controlled, such as strain sensors, floor and wall heaters, or carbon filled concrete. Reinforcement materials, such as steel meshes, could also be automatically deployed to reinforce concrete structures. Other reinforcing options are glass or carbon fibers in plastics and can be feed through the extruder head during printing [8].

To demonstrate the scalability of the CC system, Khoshnevis uses a conventional construction technique for creating concrete walls, using the CC system. Conventional practices for creating concrete structures involve using a form, comprised of sheathing, studs, wales, ties, and bracing. However, the CC system can print an outer shell of the wall section in layers, and then fill the mold after the wall has cured. Ties were added manually every 12 inches horizontally, and 5 inches vertically to add strength to the structure. Using CC, the form design and build process is much simpler, saving time and extensive effort that would normally be required for a team to manually build up forms and lay concrete [9].

Future colonization of extraplanetary bodies will require new materials that can be easily used for forming structures that do not rely on water-based concrete. A study by Lin Wan et. al. from Northwestern University in Illinois [10] showed a potential new material which they called Martian Concrete (MC). Using sulfur and a Martian Regolith

simulant, the mixture is heated until the sulfur melts and is mixed uniformly throughout the regolith. Using molds, samples were made to be tested under unconfined compression, notched three-point-bending (TPB), and splitting tensile tests. Optimal mixtures of 50/50 wt. of regolith and sulfur were observed to have a maximum compressive strength of 50 MPa or greater. The TPB tests show an average Modulus of Rupture value of 7.24 MPa. Other benefits of MC are the quick curing times, only requiring the sample to cool to reach maximum strength, as well as the ability to recast samples. The sulfur can and will melt if heated properly and can be mixed with other samples to get fresh material. After microscopy tests, it also appears that the sulfur reacts with some metal elements in the regolith simulant to form sulfates, increasing strength.

Taking the MC work from Northwestern and applying it to 3D printing, Khoshnevis has demonstrated a system called Sulfur Concrete Contour Crafting (SCCC) [11]. This system combines the CC printer previously developed, with the novel material from Wan to create a machine capable of printing using sulfur as the base cement. Using a 6-axis robot arm, and a novel extruder design, the printer can create small scale domes and special contoured surfaces. There were issues in development because of the material. This required a unique design of the extruder system using knurled rollers, rather than an auger mechanism. This lessened the impact of the material abrasiveness and reduced wear on parts, while still being able to effectively print material [12].

As 3-D printing, especially large-scale 3-D printing, is a relatively new area of research, there are limited standards for determining success of prints. Many standard plastic tests can be applied to 3-D printed parts, as shown by Letcher et. al. [13]. However, this test method gets strength properties of 3-D printed parts which, while

important, does not necessarily reflect success of the print, and print quality can be subjective. Even at the desktop print-size, parts and layers can be deformed and be inconsistent. These deformities are likely to be magnified as print size and layer size increases. To address this issue, Kazemian et. al. outlined an experimental test frame for determining print quality through experimental prints [14]. Using ASTM C150 Type II Portland cement, and three other mixtures with additional additives, printed concrete was tested according to the test frame, involving print quality observations (tearing), square edges, and dimensional precision. The shapes stability (in given time frame) of the print was also analyzed. Using the test methods, an accurate comparison between the four materials was achieved and demonstrates a reliable experimental setup for determining print quality.

Further research by CC on print quality involved studying aggregate size, extrusion rate, and layer thickness and their effects on layer adhesion and structural strength [15]. Using a control mixture, and four different mixtures with maximum aggregate sizes of 3/32", 3/16", 1/4", and 1/2", the strength was found to increase with decreasing maximum aggregate size. Extrusion rates and layer size were tested together, using three different layer sizes in a 4" cube. Results indicate higher bond strength as layer height is increased, and more time passed between layer extrusion. However, the compressive strength of the sample increased when the layer height decreased, and the time lapse between layers was short.

Using ultra-high-performance concrete, Gosselin et. al. printed freeform structures using a 6-axis robotic arm. Using a tangential continuity method to print in a true 3D sense, the group created stronger layer bonds for free form structures with

overhangs. The cement mixture consisted of 30-40% wt. Portland Cement, 40-50% wt. crystalline silica, 10% wt. silica fume, and 10% wt. limestone filler. When mixed with a small amount of water, the mixture forms an ultra-high-performance mortar paste. Flexural testing of samples after 90 days resulted in a flexural strength of 14.3 MPa. The researchers estimated compression strength based on flexural strength and water/concrete ratio to be greater than 120 MPa. Using this mixture, and the robot arm the team was able to make complicated freeform structures with curving and sloping walls that would normally require extensive formwork [16] .

A potential for construction on the Lunar surface uses a laser to melt and fuse a Lunar simulant together to create a solid structure. The process is a little more complicated as the particle size, and layer height must be compatible with the diameter of the laser to ensure a proper melt and powder packing during deposition. After experimentation using a lunar regolith simulant, optimal setting for various laser parameters and print speed were found and were used successfully to print small samples using the simulant [17]. Research beyond initial testing and optimization is lacking and need more study before viability can be determined.

Polymer concrete (PC) uses a polymer resin as a binder in an aggregate to form a concrete substance without water. Commonly used polymeric resins are polyester resin, epoxy resins, and furan resins. Bedi, Chandra, and Singh provide a review of various polymer concrete tests done by researchers and a brief discussion of findings. Some highlights include epoxy resins generally proving to have better mechanical properties, aggregate choice is mostly dependent on availability and price rather than strength

differences, and a seven day cure time is generally used and has been widely adopted through various researchers [18].

One reason PC has not been widely adopted, despite being stronger and more resistant to corrosion, is the higher cost of materials compared to standard concrete. A large supply of recycled polyethylene terephthalate (PET) has led to unsaturated polyester resin being widely used as a binder. Byung et. al. compared fresh aggregate to recycled aggregate in a PC made from recycled PET. The concrete is made using four components: the polymer resin, a filler material, coarse aggregate, and fine aggregate. The coarse and fine aggregates were combined using varying amounts of natural and recycled aggregate to observe mechanical properties of several mixtures. For example, one mix used 9% resin, 9% filler material, and 82% aggregate composed of a 30/70 ratio of natural/recycled coarse aggregate, and a 30/70 ratio of natural/recycled fine aggregate. The researchers also varied the amount of resin and filler used, 9, 13, 17%, while varying the aggregate content and composition. Results show that compressive strength generally decreases as recycled aggregate content is increased. Similarly, strength decreases in flexural and split tensile tests as recycled aggregate is added. At a resin content of 13%, the overall strength increased, but a decreasing trend with increasing recycled aggregate was still observed. At 17% resin content the strength did not show significant change despite addition of recycled aggregate, indicating a higher resin content could make up for the decreased strength of recycled aggregates [19].

Another study, by Mahdi, Abbas, and Khan, studied the effect of different resin compositions and manufacturing methods on mechanical properties. The researchers used unpurified, recycled PET bottles and used different combinations of glycol ratios, dibasic

acids, and initiator promoter combinations to make eight sets of polymer mortar (PM) and PC. The PET to glycol ratios were 1:1, and 2:1 for all groups. The other major difference is in the initiator promoter combinations. Two groups used were Benzoin peroxide (BPO) and N-diethyl aniline (N), and Methyl ethyl ketone peroxide (MEKP) and Cobalt naphthenate (CoNp). The PM mixture was cast in to 70.6 mm cubes, while the PC mixture was cast in to 150 mm cubes and 150 mm tall, 75mm diameter cylinders. General trends differ between the results for PM and PC, but generally a 2:1 PET to glycol ratio was stronger and using MEKP as the initiator produces samples with a higher compressive strength. However, the strongest samples do not come out of the same group. The highest strength PM used a different dibasic acid than the highest strength PC group. Tensile strength in the PC samples was similar or greater than that of comparable grade concrete. The study also concluded that the PET used did not have to be purified, which simplifies the process and lowers cost [20].

CHAPTER 3: METHOD AND APPROACH

Development of a 3-D Printer capable of printing materials used was done alongside the material selection process, with much of the design outlined in section 3.1. For all materials, strengths were compared to standard compressive and flexural strengths of residential concretes of 20-40 MPa, and 3-5 MPa respectively [21]. The goal of building material selection was to use materials that would be easily sourced locally or would be waste products from cargo or manned missions to a planetary body. Sulfur was an option, as sulfur is readily found on Mars. There are also several polymers that would work as well including Polyethylene Terephthalate (PET), and High-Density Polyethylene (HDPE). The polymers could be used for food storage, supplies, and equipment storage and repurposed as a construction material.

3.1 Test Printer Design

To test material printability, a large table top printer (see Figures 1-3) was designed with the intention of printing small samples for strength testing and print quality observations. The overall design is identical to a typical Fused Deposition Modelling (FDM) printer, with the notable exception of the extruder design. The main printer structure was designed using Solidworks [22], and is comprised of 1.5 inch aluminum extrusion, and linear bearing rods. The large cubic area is the print area, and the top to structures are support for the large extruder tube and motor. The extrusion system uses a NEMA 34 motor to turn a 2-inch earth auger which pushes material through the nozzle, which differs from a conventional motor and gear system that feeds plastic filament. Four

700W heater bands wrap the extruder tube and provide the energy for heating material. Some material tests required a steady state temperature of 300C, and the heater bands and control were easily able to maintain temperatures. The 3D printer control system uses NEMA 23 stepper motors, controlled via Repetier-Host [23] using a Ramps 1.4 shield mounted on an Arduino Mega 2560. This control setup is common for homemade printers and has been used extensively.

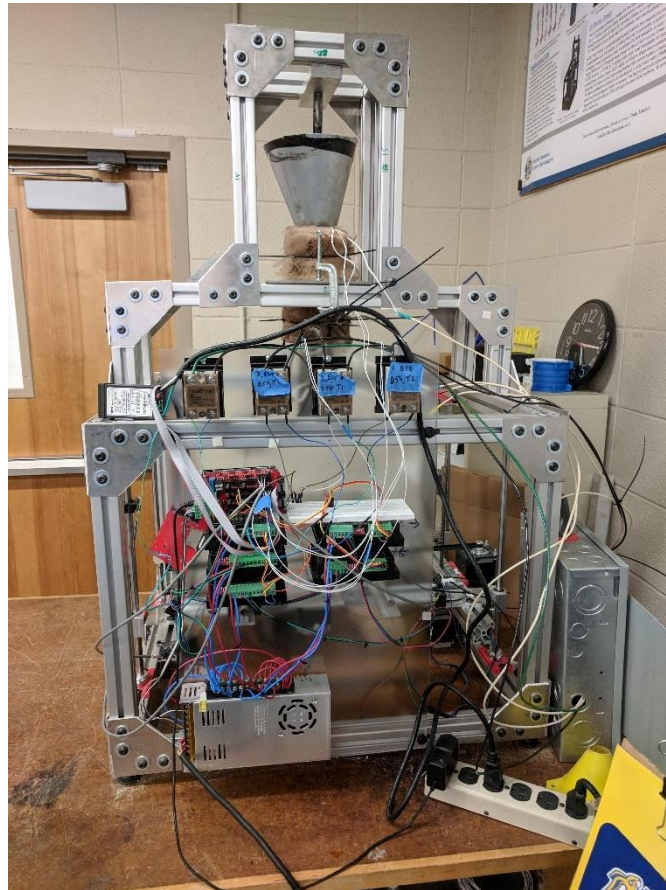


Figure 1. Test Printer Controls

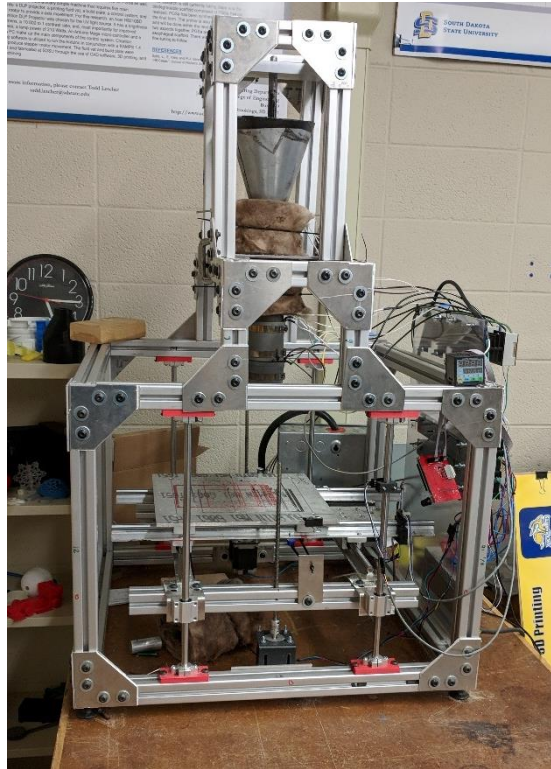


Figure 2. Test Printer Front View

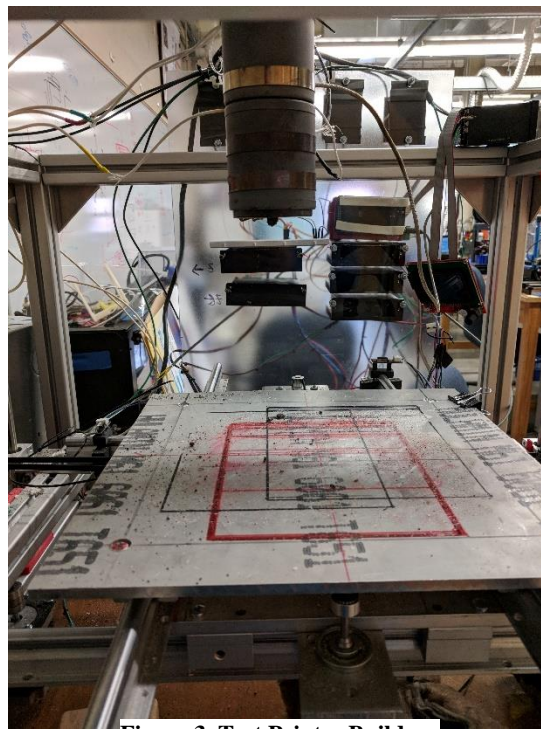


Figure 3. Test Printer Build Area

3.2 Material Selection

Early work on development of a material used the sulfur-based material developed by Northwestern. Initial work was promising, using molds and a hot plate to melt, mix, and form cylindrical and rectangular samples for testing. However, a potential safety hazard of overheating the material causing auto-ignition of the sulfur proved the material to be dangerous to use for practical applications. A brief test of a premixing system, and an attempt at extrusion for printing also showed the difficulty and hazards associated with a sulfur material. The work was not without positives though, as a small sample was very roughly printed using the sulfur concrete, shown in Figure 4.



Figure 4. Printed Sulfur Sample

The molded samples of sulfur concrete did not perform as well as the Northwestern research, and the strengths achieved were slightly lower when compared to residential concrete, achieving a compressive strength of 18.6 MPa, and a flexural strength of 1.7 MPa. These results coupled with the difficulty and hazards of working with sulfur pushed the decision to switch polymer bases.

Next, a review of the rules for the NASA 3DPH Challenge showed NASA's preference in using materials for a structural habitat. The chart showing the scoring system for the 3DPH Challenge is shown in Figure 5.

Material Applicability	Earth Relevant					Mars Relevant				
	Aggregate	LD	MG			SS			GS	BSR
Polymers (including fibers)	MR, EVOH	NY, PU	PT, ABS	S	PS, PC	PMMA, PET, PETG	PLA, PVC, VY	BR	PP	PE (HD and LD)
Additives	FP	AM	SC					A		B
Binders	PG	HA	IW					GST		MBC
3DP Factor	1	2	3	4	5	6	7	8	9	10



Figure 5. NASA Challenge Material Score Sheet

The first polymer considered was PET for its high strength and the versatility. However, shortly after print testing this material it was found that PET becomes brittle after re-melting and is cooled. Research in to PET was discontinued at this point to avoid potential future strength issues. Also, the melting point of PET is very high – around 280C – and would have required a significant amount of energy to melt efficiently. When taking the future goals of making a system to be used on other planets in to consideration, the high energy cost was a major deterrent for the selection of PET.

The other polymer considered was HDPE, which was the highest ranked material choice according to the NASA 3DPH Challenge. HDPE is also quite strong and versatile, but with a lower melting point of around 160-180C. HDPE also does not become brittle after melting. One major downside is the viscosity of the material. However, using an

auger to extrude material, would make the process easier, provided the motor had enough torque to rotate the auger. Since the intention was to use HDPE as the base 'cement' for the material, it would have to be imported and not readily available on another planet. The best source for HDPE would be to use it for packaging of supplies. Large crates for storing bulk goods, as well as the individual packaging for most of the supplies would be the most useful way to get the HDPE to another planet.

The last piece of material to choose was the aggregate. In the sulfur concrete, a Martian regolith simulant was used. This simulant could have been used as well, however it was expensive and difficult to get in bulk quantities need for the 3DPH Challenge. The list of materials NASA provided included aggregates of various types from limestone and marble, to basaltic sedimentary and crushed basaltic igneous. For ease of purchasing and availability, siliceous sedimentary rock, or simply sand, was chosen. Initial sand aggregate of less than 5mm was used, and designated coarse sand (CS), but as research progressed the need for a smaller, consistent particle size became clear. A second sand aggregate of less than 2mm was also used, designated Fine Sand (FS). There was no mixing of coarse and fine sand for use in testing, mostly because the future printer design was meant to be as simple as possible and using different aggregate sizes and ratios would be difficult to do autonomously. All samples were made using either CS or FS, and HDPE.

3.3 3D Printed Habitat Challenge Printer

The 3DPH Challenge was the main motivation for this research and much of the decision making and development was geared towards the competition. The end goal of

Phase 3 is to print a 1/3 scale habitat, that each participating team must design. There are other levels along the way involving habitat design and virtual construction, as well as physical construction, but the focus of research has been done on the material itself. The competition focuses on using recycled materials from missions, and other locally available resources to produce habitats. Early test prints on extrusion showed the small test printer was not going to work for the particle size, and sample size that would need to be printed. This occurred around the announcement of Phase 3, when a student team from South Dakota State University (SDSU) was formed to design, build, and operate a large-scale 3D printer that would print the thermoplastic concrete being developed. While the printer and competition itself is not the focus of this research, it is worth mentioning as it is the inspiration and driving force behind the material development and future work.

From the NASA rules, the habitat needed to have a living space of a minimum of 93m² for four astronauts. After reviewing the habitat criteria and much deliberation on printer structure design, habitat layouts, and the realistic goals the team could achieve, a final habitat design with a 13.5x9m footprint became the end goal. At 1/3 scale this meant the printer would need a print bed of 4.5x3m. The scaled habitat would also be at max, 1.5m tall so the print head needed a travel range of at least that much. With this massive print size, unique adaptations were needed to printer designs to be able to control the printer by simple software, while still meeting all the requirements of the challenge.

The extrusion system is nearly identical to the original test printer, with a slight upscale to heat and extruder material faster. A larger NEMA 34 motor with a peak torque of 1600 oz.-in. was used. Part of the issue with the small test printer was that there was a significant amount of back pressure on the auger that was not anticipated, which meant

the motor was receiving a lot of axial force, but for full torque and proper operation, it should not be receiving this additional force. To fix the issue, an auger coupling shaft mounted in a thrust bearing was set in to a block of aluminum. This block would be mounted to the head frame separate from the motor mounting to prevent any axial force beyond the auger. To increase torque further, a sprocket-and-chain system from the motor to the auger was used to increase the torque in a 1:4 ratio. A longer 2-inch auger was used inside a 28-inch extruder tube. Five 700W heater bands heat the main tube length, and a 500W heater band heats the nozzle. A view of the Solidworks model is shown in Figure 6.

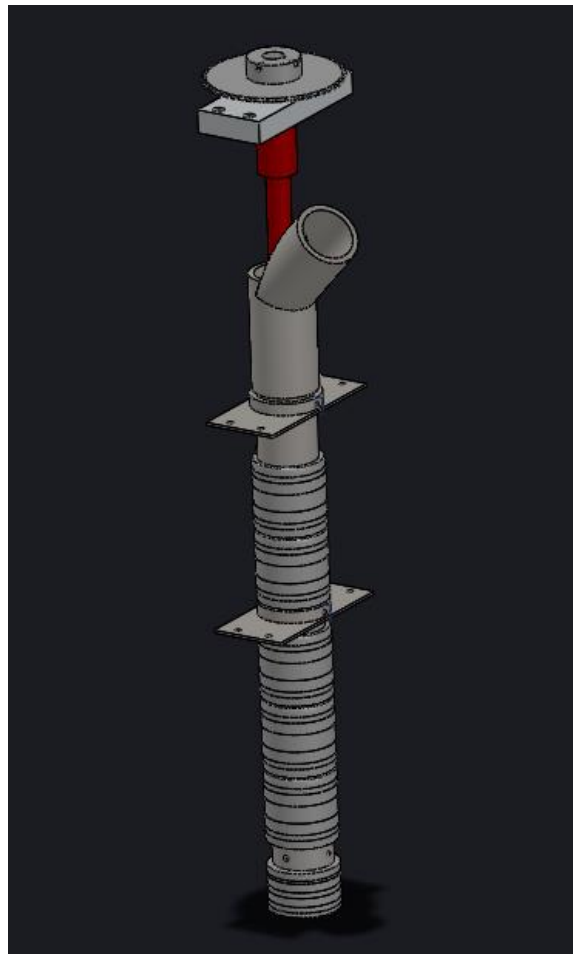


Figure 6. Extrusion System Model

The superstructure of the printer resembles a small rolling crane, with four legs joined by gusset plates make up two towers to support an overhead beam. The base is wider than the main column of the tower to provide extra stability when traveling and is four feet wide. The beam across the top, referred to as the Y-axis, used two pieces of angle supporting the weight of the print head. Early in the design process there was concern over the deflection on the Y-axis beams. Beam deflection calculations were done for a variety of beam sizes and profiles. The print head was estimated to weigh 250 pounds. To provide multiple factors of safety, the print head was assumed to be 500lbs, and the weight would be supported by a single beam only. After calculating and comparing options, an angled aluminum beam of half-inch thick aluminum would only deflect 0.1456 inches. Since there would be two beams, the deflection would be effectively halved. Motion is achieved using a unique rail and cart system, and a rack-and-pinion system is used to drive the print head. The overall width is then 13.5ft, or 4.11m which gives plenty of room for the wide print head to reach that 3m print width. Figure 7 shows a Solidworks view of the super structure, and Figure 8 shows the cart system.

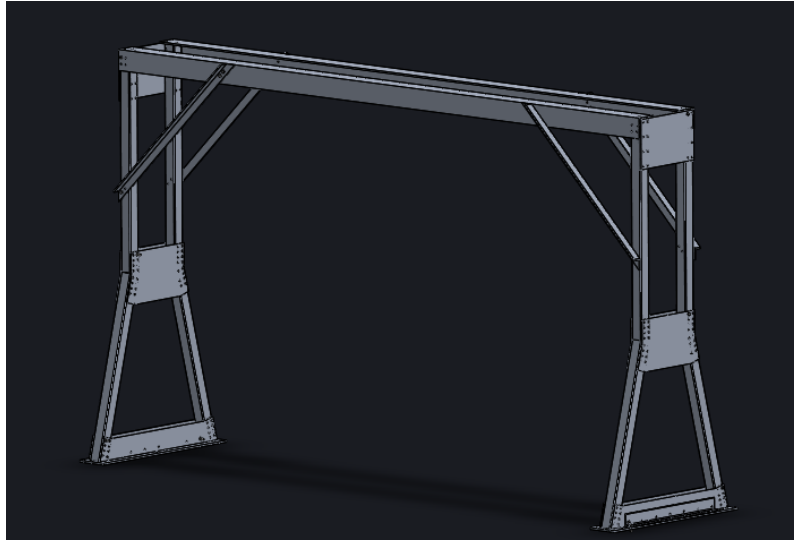


Figure 7. Superstructure Model

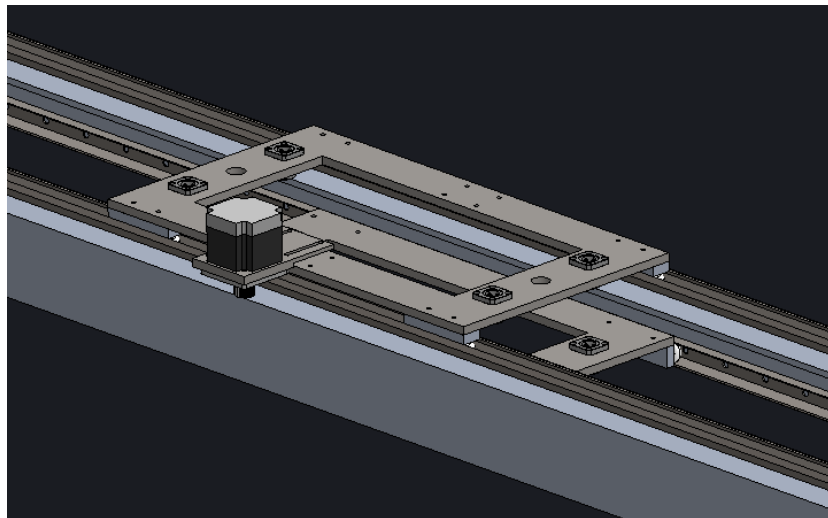


Figure 8. Y-Axis Cart System Model

The most difficult part of the X-axis was finding a way to keep a straight motion down the full length and finding a roller or track system to support the weight of the printer. V-groove caster wheels were a viable option and could easily support the weight spread over six wheels; however, to keep the motion straight they need a ‘V’ shape to follow. A unique solution using a U-channel with two angles welded to the inside makes

up the rail on both sides of the printer was used and allows for straight line motion. The drive system for X-axis motion is identical to the Y-axis, using a rack-and-pinion system, but with two motors, one on either side. The rack is mounted to the outside of the U-channel. The X-axis needed to have a 4.5m length at a minimum, but with the wide base to provide the rail needed to be at least 18ft. long. Since U-channel and angles were easily available in 20ft. sections, that length was used to provide plenty of area for motion without getting dangerously close to the ends of the X-axis. Figure 9 shows the super structure mounted on the X-axis rails, and Figure 10 shows a view of the X-axis rail.

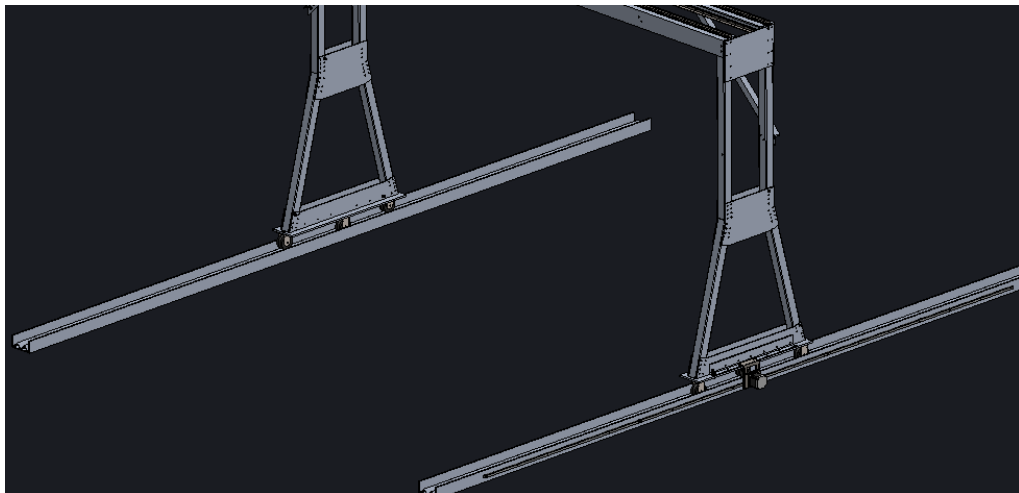


Figure 9. Superstructure Mounted on X-Axis Rail

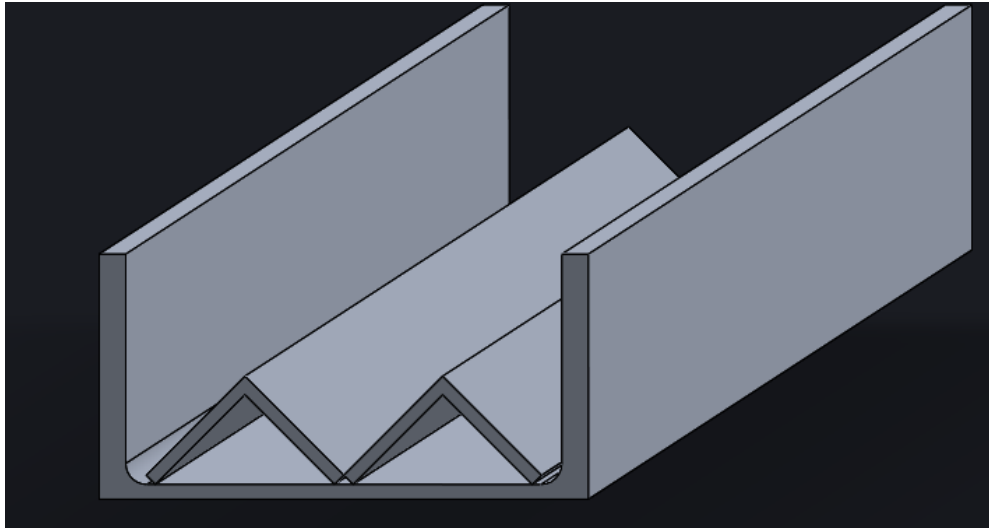


Figure 10. X-Axis Rail Design

For the Z-motion, two lead screws were implemented with the nut from the screws secured to the bottom plate on the dual track of the Y-axis. The lead screws passed through the upper plate on the Y-axis and mount on a plate at the top of the print head structure and at the bottom where the extruder was mounted. The print head is raised and lowered on the Y-axis rail. The central structure of the print head is made from aluminum extrusion to provide more rigidity than just lead screws would. Four hardened ground steel rods provide a moment reaction to some of the swaying. The rods pass through bushings in the Y-axis cart plates. The print head is raised and lowered by a NEMA 34 motor mounted to the top plate, with a sprocket and chain system to move both the lead screws at the same rate. The total travel height of the printer is about 2.4m, however the 1/3 scale habitat will be 1.5 m at max. Figure 11 shows a view of the print head, and Figure 12 shows the full printer assembly.

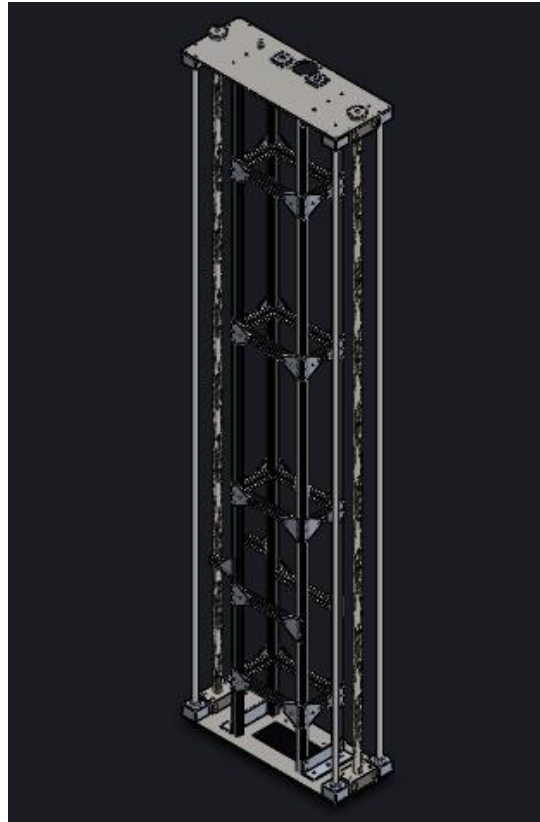


Figure 11. Print Head Structure

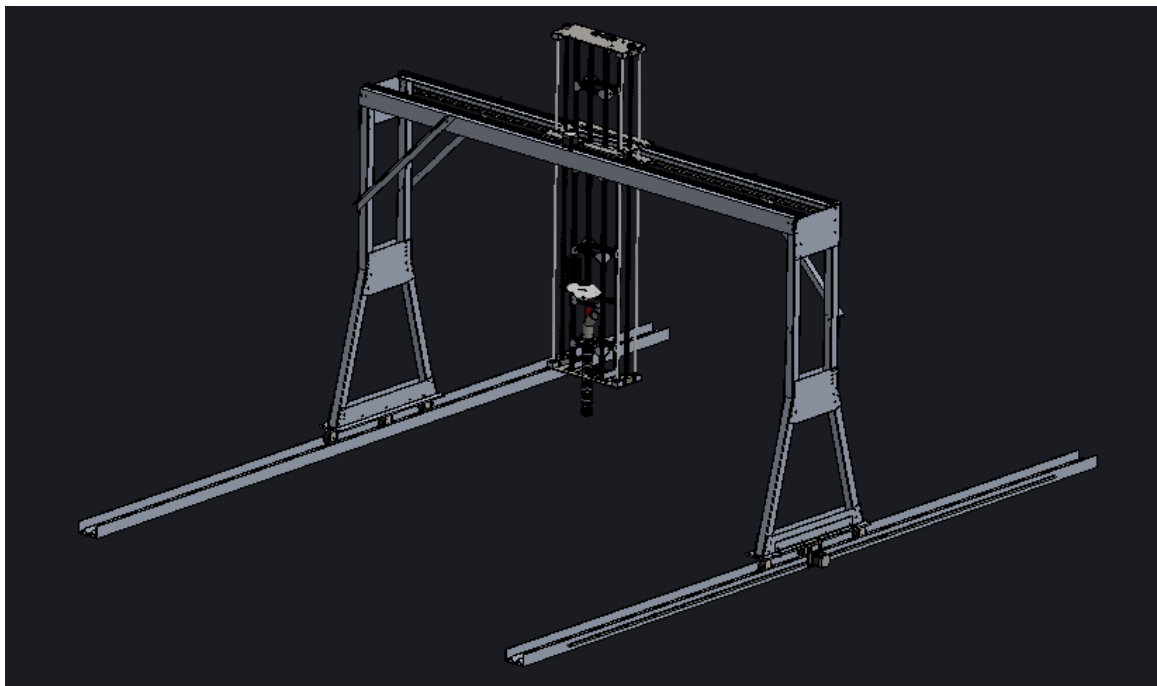


Figure 12. Full Printer Assembly

3.4 Molded Sample Test Plan

Having chosen a material to use, a test plan was developed to determine an optimum mixture ratio of plastic to sand. Since the goal of the 3DPH Challenge is to use minimal imported material, a ratio range of 20-50% plastic by weight would be sufficient for strength testing. In increments of 10%, plastic was mixed with the two different grades of sand for a total of 10 batches of HDPE/sand mixes. The material was then placed in an oven at 215C until the HDPE thoroughly melted. No mixing during the melt process took place. A batch of 100% HDPE was also manufactured to use as a measure of pure polymer strength. Figure 13 and Figure 14 show mixtures for flex and compression samples in molds after being melted.



Figure 13. Melted Flex Samples in Molds



Figure 14. Melted Compression Samples in Molds

To start, two samples each were made of 20-50% plastic with the coarse aggregate to get a rough idea of the strength ranges so a preliminary decision on mixture ratios could be used to go forward with printer design. Later, six samples were made for each batch, but in some of the lower plastic content samples, flex samples were broken during removal, so the final sample count is lower.

3.5 Flexural Testing

Due to non-conventional nature of the material, (HDPE and sand aggregate), there are no ASTM testing standards that exactly match and specify testing methods. However, because the samples were made from a rigid plastic matrix material and failures closely approximated rigid plastic failures, so flexural testing was performed and calculated according to ASTM D790 Standard Test Methods for Flexural Properties of Unreinforced

and Reinforced Plastics and Electrical Insulating Materials [24], with a few exceptions. The first is regarding the shape of the sample, and the second is the span distance. Both of these changes were taken from ASTM C78 Flexural Strength of Concrete [25]. ASTM C78 calls for a span of three times the height of the specimen, with at least a 25mm overlap on each side. The flex sample size was then 1 inch tall, by 1 inch wide, by 6.5 inches long. This gave plenty of length to work with and allowed a span of 75mm, or about 3 inches to perform 3-point bending tests.

Molded samples were formed at 1x1x6.5 inches but needed to be faced flat on the top side after cooling. Because of the facing, the samples were shorter than they were wide, so testing was done edgewise to maintain a height of about 25mm, so the span could stay 75mm. Samples were displaced at a rate of 1.3mm/minute. Testing was completed at the South Dakota State University METLAB on an MTS Insight. An example of the flexural testing setup shown is in Figure 15.



Figure 15. Flexural Test Setup

3.6 Compression Testing

Sample were also made to be tested in compression according to ASTM D695 Standard Test Method for Compressive Properties of Rigid Plastics [26]. The samples were originally molded to 25.4mm by 50.8mm, however deformities in the upper region of the samples needed to be removed to have a flat testing surface. Unfortunately, this meant facing nearly 20mm off the samples to get a clean surface. Due to the smaller sample it was more difficult to determine an actual failure point for the sample, but failure was eventually determined by visual observation of the material. Significant deformation resulting in surface stress cracks usually occurred around the five-minute mark and was considered the point of failure for the samples. The failure point is not the most relevant information, rather, the compressive yield strength. For ASTM D695, compressive yield strength is determined by the deviation from linearity on the stress-strain curve by a specified percent of deformation, which for this research was selected to be the generally accepted 0.2% offset. Figure 16 shows a sample in an MTS Landmark.



Figure 16. Compression Sample in Test Fixture

3.7 Printed Sample Quality Testing

After testing molded samples and determining the best ratio/strength combination for the challenge. Qualitative tests of the print quality were performed to find a suitable mix of parameters by changing feed rate and steps/mm of the extruder, print speed, and layer heights to make high quality printed samples. Steps/mm for the extruder is not a typically altered parameter for printing, however the material is not pure plastic, and the extruder tube is much larger than the nozzle opening so a direct ratio of revolutions to material deposition is not easily defined. Initial printing was done a piece of particle

board to help prevent rapid cooling, and for easy removal of prints. A view of the temporary print bed, and extruder is shown in Figure 17.

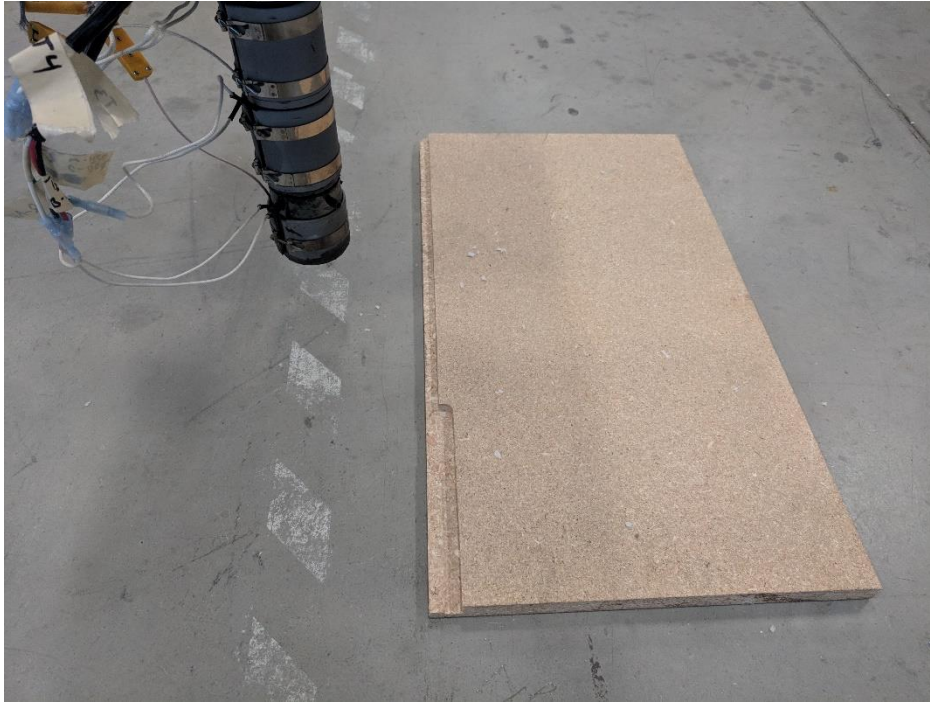


Figure 17. Test Printing Setup

The test prints attempted to make rectangular beams that could be used for thermal cycle testing. Most print tests were cut short, especially early on because print quality was easily lacking from the start. As the parameters changed and quality improved, the print process went on longer until full parts were printed. An example of a good quality print in process is shown in Figure 18.



Figure 18. Printing Tests in Progress

3.8 Printed Sample Strength Testing

As printing and the 3DPH Challenge continues, strength testing will need to be done according to ASTM concrete standards using much larger parts, but this was outside the scope of the initial material research. Strength testing on the printed samples was initially done to verify that the print became one homogenous part instead of distinct layers. It was also a way to verify the mixture ratio coming out of the nozzle. Material was manually mixed and loaded in to the extruder before printing in the correct ratio, but

it was unknown how the material moves through the extrusion system and whether the ratio remained the same. The sand tended to settle through the HDPE during measuring and mixing so there was the potential for separation.

Flex and compression samples were cut from unused samples of the thermal cycle samples to a similar size of the molded samples to get a more direct comparison. Compression samples for printed parts were cut to 1x1x2 inch blocks instead of cylinders. As allowed by the ASTM testing standards, the samples were cut from larger prints to maintain dimensional consistency. The print process is not perfect on a very small scale, so the sample layers would occasionally not be correctly positioned, and certain layers would be thinner, or wider in some cases. To minimize this surface effect, the prints were cut in to smaller sections, samples of which are shown in Figure 19.



Figure 19. Flex Samples Cut from Printed Block

CHAPTER 4: RESULTS

Testing produced a variety of results characterizing the thermoplastic concrete. X-ray inspections showed distribution and density comparisons of samples. Strength testing yielded a variety of results for different mixture ratios. Printing was successful, and samples were also tested and compared to the previously molded samples.

4.1 Digital Radiography Inspection of Molded Samples

The molded samples were faced after cooling to get flat faces all the way around for accurate measurements. The samples were inspected by digital radiography to see the internal material structure. This was done to check for air bubbles inside the parts that would affect strengths, as well as to verify the sand does not settle during the melt process. The pure HDPE samples were the first to be inspected. Since they are just pure HDPE with no aggregate, the samples were only inspected for major air bubbles. A radiograph is shown in Figure 20 with several flex samples. For the most part the samples are solid, with minor voids in the center, and a few extra particles of foreign debris.

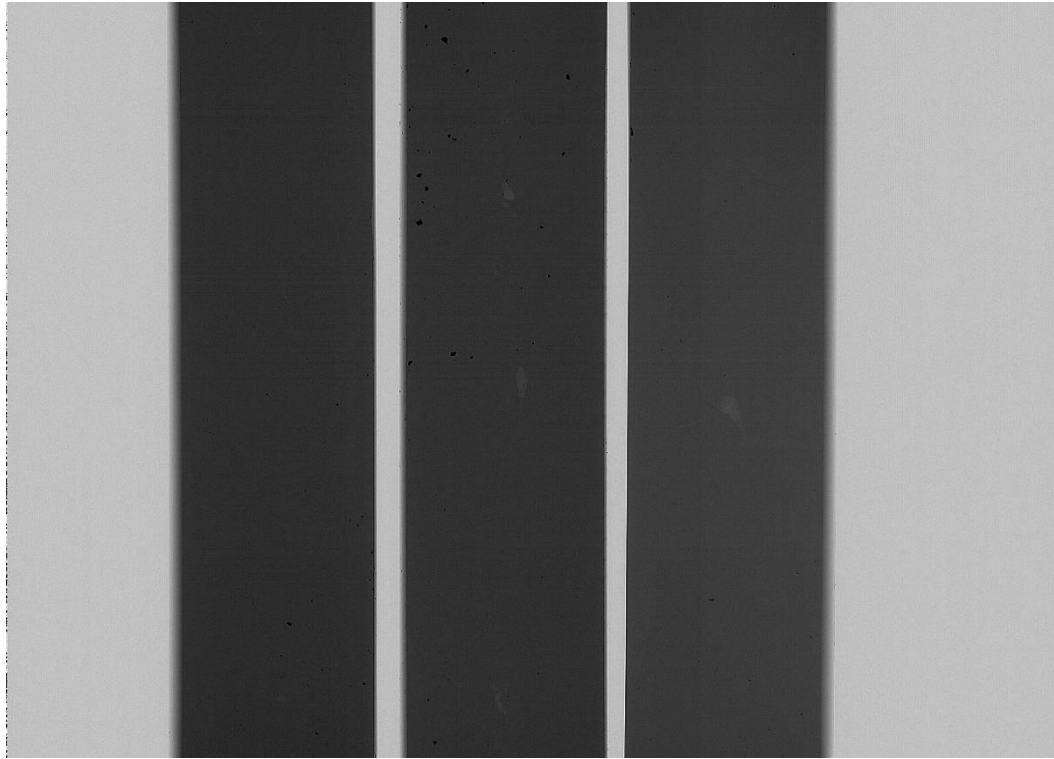


Figure 20. Radiograph of Pure HDPE Flex Samples (Left to Right 1,2,3)

The pure HDPE compression samples had more air voids, especially in Sample 1. The first three samples created are shown in Figure 21. The presence of air voids was noted to improve the sample manufacturing process in the future. All other samples were removed from the oven, and the melted mixture was packed, and more material was added to remove as many air voids as possible.

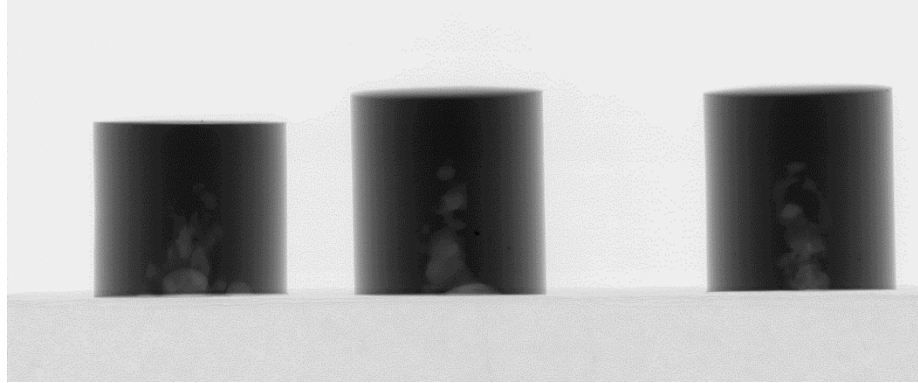


Figure 21. Radiograph of Pure HDPE Compression Samples (Left to Right 1,2,3)

The other objective of radiograph inspection was to verify that the sand does not settle during the melt process. Figure 22 shows a side view of samples 1-6 of 30% HDPE/CS flexural specimens. From the figure, it clearly shows an even distribution of sand throughout the samples. Figure 23 shows samples 3-5 of 30% HDPE/CS compression specimens, which show a similar sand distribution throughout.

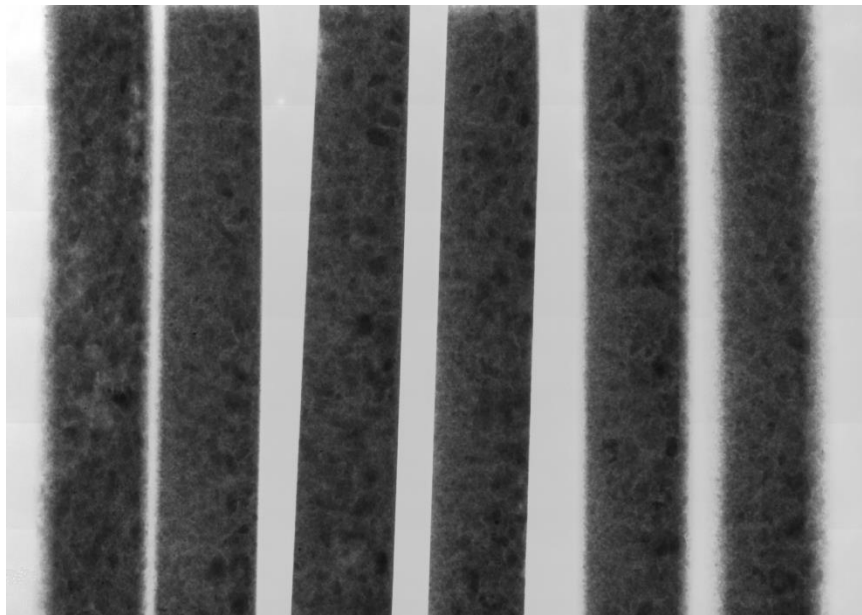


Figure 22. Radiograph Side View of 30% HDPE/CS Flex Specimens (Left to Right, 1-6)

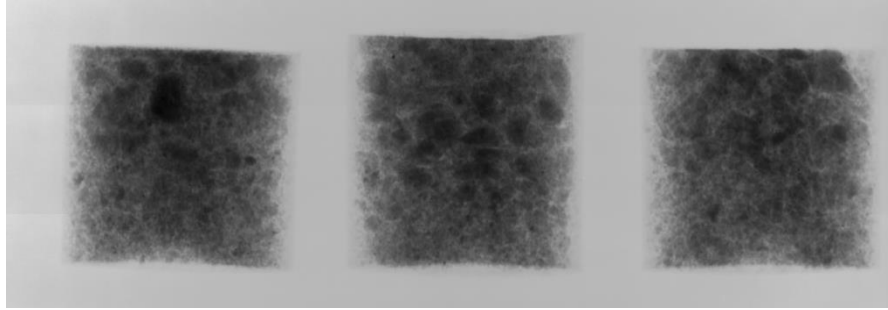


Figure 23. Radiograph of 30% HDPE/CS Compression Samples (Left to Right, 3-5)

Figure 24 shows flex samples of 20,30,40 and 50% plastic side by side in a single radiograph. It is highly evident that each one is significantly different, despite only having 10% more plastic by weight from sample to sample.

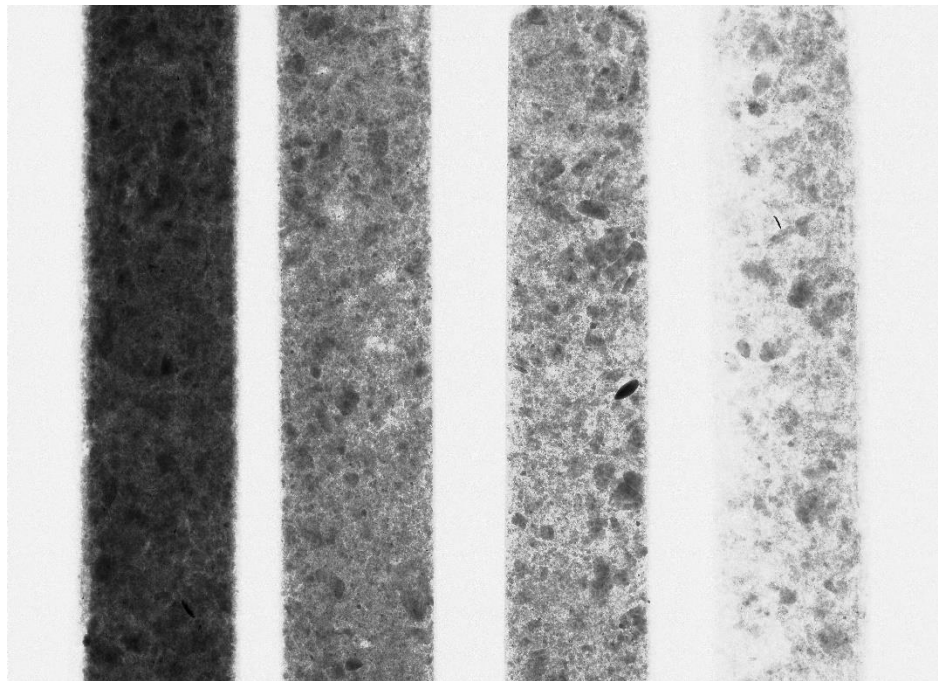


Figure 24. Radiograph Comparison of (Left to Right) 20, 30, 40, and 50% HDPE/CS Mixtures

4.2 Flexural Testing Results

Flexural testing failure was defined as tearing on the bottom side of the beam at the rupture point, an example is shown on a 50% HDPE/FS sample in Figure 25. Load and displacement was collected throughout the test and a short program in MATLAB calculated stress-strain curves, and all other flexural mechanical properties. The stress strain curve was then used to determine the maximum stress, or Modulus of Rupture, and to determine the Modulus of Flexure by calculating the slope in the initial linear elastic region. The Modulus of Flexure is also used generate another line using a 0.2% offset to determine the yield stress. A representative stress-strain curve from the same 50% HDPE/FS sample is shown in Figure 26. On the left is the standard curve, and on the right, is the curve with a fit line in the linear elastic region.

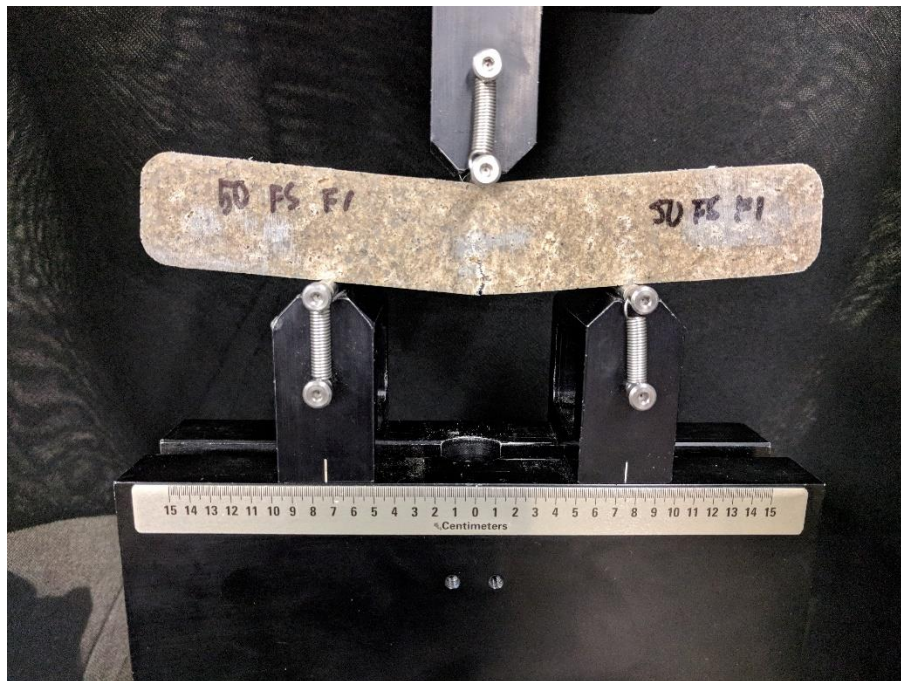


Figure 25. Flexural Failure of 50% HDPE/FS Specimen

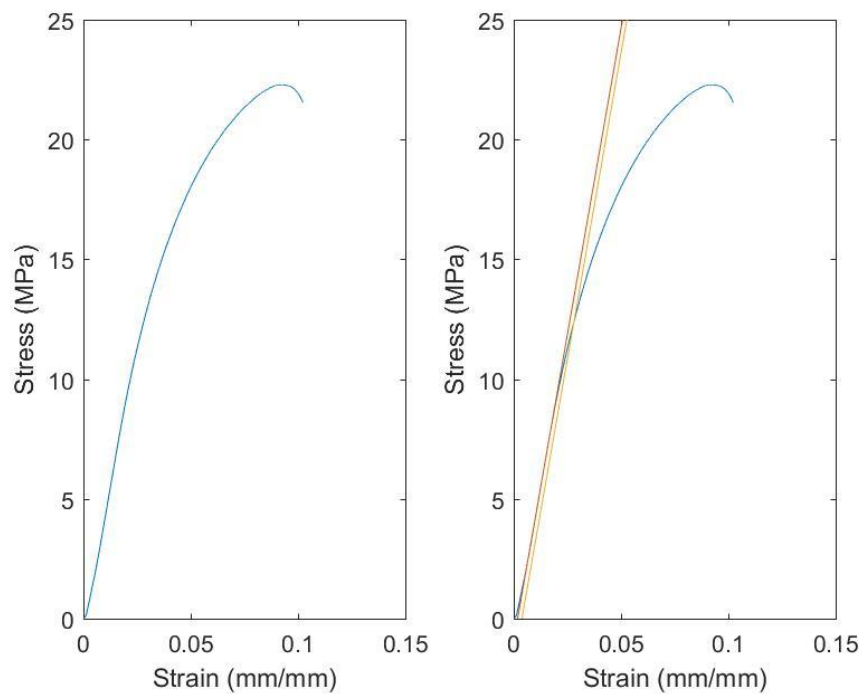


Figure 26. (Left) Stress Strain Curve for 50% HDPE/FS Flex Specimen (Right) Stress-Strain with Modulus of Flexure Fit Line

The maximum load is the Modulus of Rupture; however, Yield Stress is perhaps the more important piece of information. Pure HDPE was tested first and has a flexural yield stress ranging from 18.73-22.28 MPa, with an average of 20.23 ± 1.16 MPa. The Modulus of Rupture, however, had an average of 43.02 ± 4.11 MPa, showing that HDPE can experience significant amount of yielding before finally breaking. Either way, pure HDPE is much stronger in bending than concrete, which typically ranges from 3-5 MPa. When mixed with CS the Modulus of Rupture and Yield Stress vary by a much smaller amount but decreases as the plastic percentage decreases.

FS tended to lower the average flexural strength of the respective mixture ratio, with an exception for the 30% mixture. Even with this lowered strength, the results were more closely grouped, resulting in a smaller standard deviation. The particle size is more consistent in the FS aggregate so there is more even distribution of stress. If the stress is

distributed evenly, the failure points between samples will deviate by a smaller amount. In the CS aggregate, there were obvious particles that exceeded the 5mm max particle size, typically only in one dimension. These thin, but long particles slipped through the mesh, but ended up affecting the strength of each specimen, causing results to vary more. The only exception to a smaller deviation is the 20% HDPE/FS mixture, which had more varied results than the CS mixture. This has been attributed to a more uneven distribution of plastic because the fine particles of sand made it more difficult for melted HDPE to flow between the particles. Two 20% HDPE/FS samples were also broken during removal, demonstrating more brittleness and a lack of bonding by the HDPE.

Flexural strengths were plotted together to compare plastic percentage with flexural strength. All the CS, FS, and pure HDPE samples are shown, as well as reference values for concrete at 0% plastic. The plot is shown in Figure 27. There is a decrease in strength for each decrease in plastic percentage, which would be expected. The CS mixtures show a consistently linear decrease, drawing a nearly perfect line between concrete and pure HDPE. The FS is also linear, with a slight deviation by the 30% HDPE/FS mixture.

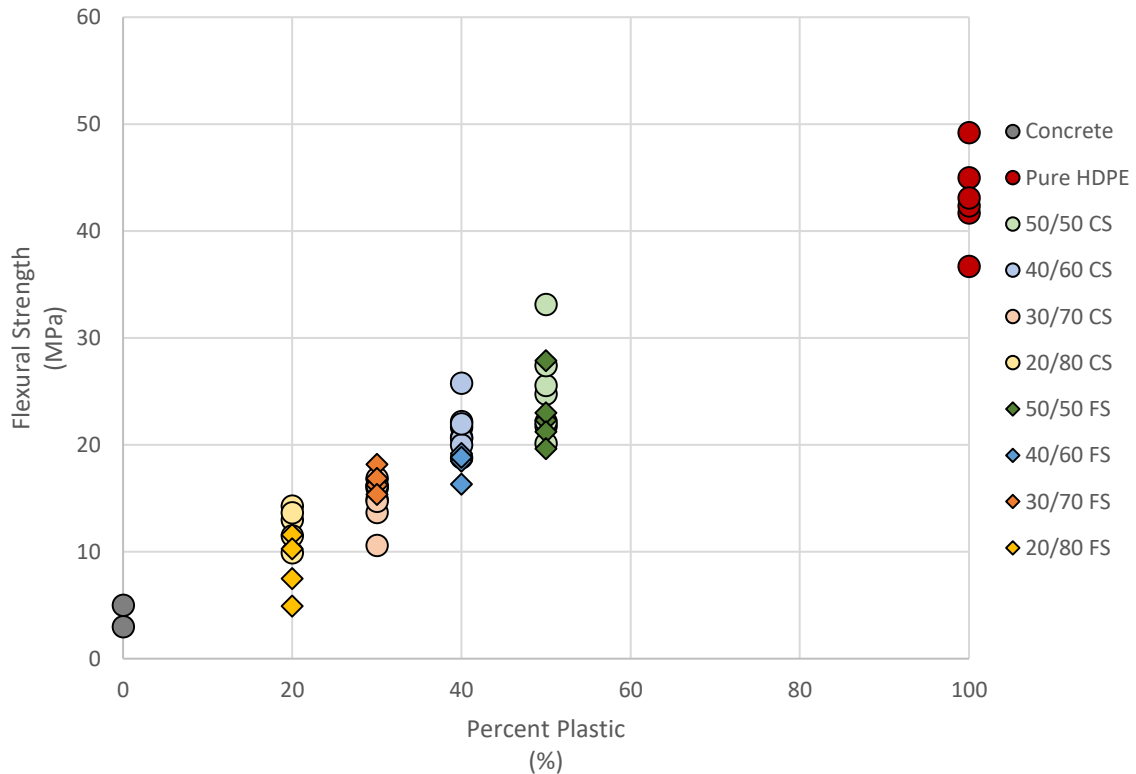


Figure 27. Graph of Flexural Strength vs. Percent Plastic

The lower strength is generally because of the lower plastic content which physically binds the aggregate together into a cohesive part. The sand has zero adhesive properties and mostly serves as a volume filler. There is not a definitive reason for the generally lower strengths of FS specimens. One potential reason is that the FS particles are smaller and clump together tighter, so plastic could not penetrate as well during melting. Since no mixing took place during the molded sample melt process, this is a likely possibility for lower strengths. These cracks would then be left open and filled with air, rather than filled with HDPE, resulting in lower strengths. Another thought follows a similar line of reasoning on particle interaction. The FS particles, again, pack together closely when stressed. In the CS mixtures, larger particles collide internally and resist

deformation until they are forced to shear apart under high loads. With the FS, instead of resisting deformation and reacting against stress, the smaller particles ‘flow’ between each other and fill in gaps. Evidence of a lower resistance to deformation is obvious when looking at the Modulus of Flexure. This value is a parallel to the Modulus of Elasticity commonly found with tensile tests. The Modulus of Flexure is the materials resistance to bending, with increasing values showing less deformation. Figure 28. Graph of Average Modulus of Flexure vs. Plastic Percentages shows a plot of the average Modulus of Flexure for all tested samples, with standard deviation error bars.

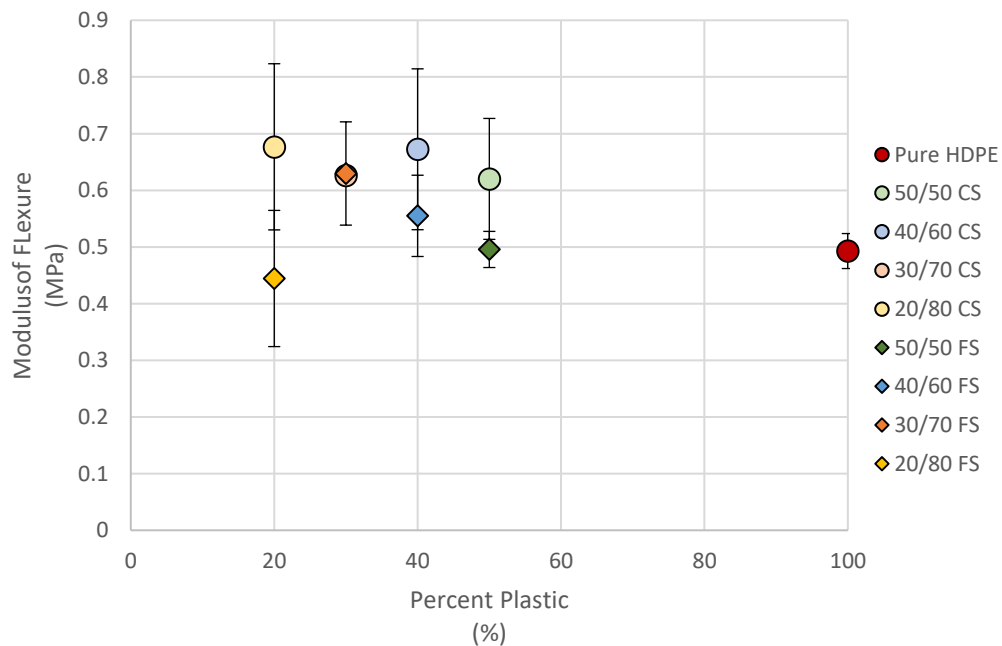


Figure 28. Graph of Average Modulus of Flexure vs. Plastic Percentage

In general, the Modulus of Flexure increases as the amount of plastic decreases because the sand particles do not deform like HDPE. Often, this can indicate a higher yield stress in parts. For this material, however, yield stress is lower because HDPE is doing the binding, and if there is not a good bond the specimen will not hold up to higher

stress. The FS mixtures also exhibit a lower Modulus of Flexure than the CS mixtures of the same plastic percentage, except for the 30% mix. Again, the 30% HDPE/FS mixture defies the trend for material behavior. This behavior for the 30% HDPE/FS mixture is thought to be due to a more even volume ratio and a consistent distribution of particles and particle sizes. The plastic and sand exists in even amounts and is well mixed so the samples behave nearly identical from test to test. For the rest of the samples, the lower FS Modulus compared to CS is more evidence that the smaller particles slide between each other rather than collide. This lack of resistance on the compressive side of the beam would allow more deformation from tension on the bottom side of the beam, meaning samples would yield and break earlier. More research is needed to verify this result.

From these flexural results, a 30% HDPE/FS mixture is likely to be the best ratio and aggregate size to use for a 3D printed habitat, and for the 3DPH Challenge. All the mixtures showed better Yield Stresses than concrete, but the 30% HDPE/FS mixture has a good balance of strength, low plastic percentage, and consistent strengths compared to the result of the mixtures. Table 1 shows a compiled list of the average Modulus of Rupture, Yield Stress, and Modulus of Flexure of the Pure Plastic, CS, and FS molded specimens.

Table 1. Average Flexural Strength Values of Pure HDPE, CS, & FS Mixtures

Mixture	Mod Rupture (MPa)	Yield Stress (MPa)	Modulus of Flexure (GPa)
100	43.02 ± 4.11	20.24 ± 1.16	0.49 ± 0.03
50% HDPE/CS	24.99 ± 4.37	16.57 ± 1.45	0.62 ± 0.11
40% HDPE/CS	21.46 ± 2.07	16.96 ± 1.3	0.67 ± 0.14
30% HDPE/CS	14.89 ± 2.01	13.73 ± 1.67	0.63 ± 0.15
20% HDPE/CS	12.47 ± 1.77	12.19 ± 1.66	0.68 ± 0.06
50% HDPE/FS	22.8 ± 3.11	13.56 ± 1.64	0.5 ± 0.03
40% HDPE/FS	18.35 ± 1.15	12.18 ± 0.63	0.55 ± 0.07
30% HDPE/FS	16.68 ± 1.02	14.03 ± 1.59	0.63 ± 0.09
20% HDPE/FS	8.57 ± 2.97	5.44 ± 3.82	0.44 ± 0.12

4.3 Compressive Testing Results

Compressive failures on plastics are sometimes hard to characterize. ASTM 695 [26] specifically addresses this for some plastics with high ductility. They do not crack or shatter like concrete does, they generally continue deform with a steadily increasing normal stress until it becomes virtually flat. There is a point where the plastic ‘mushrooms’, after yielding where the edges bow out and become circular. The true point where this starts to happen is also difficult to pinpoint and is usually based on observation rather than test measurements. For material mixtures tested, the failure point is during the mushrooming stage of the cylinder, when stress cracks, ruptures, or sand particles poke through the sides and appear on the surface. An example of a specimen after failure in a 20% HDPE/FS mixture is shown in Figure 29 with significant surface cracking. Figure

30 shows another example from a 50% HDPE/FS sample with a less obvious stress crack on the front surface, but more noticeable mushrooming.

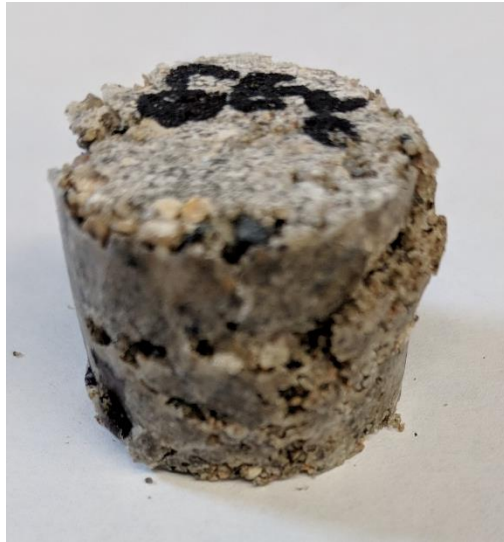


Figure 29. 20%HDPE/ FS Compression Specimen After Failure

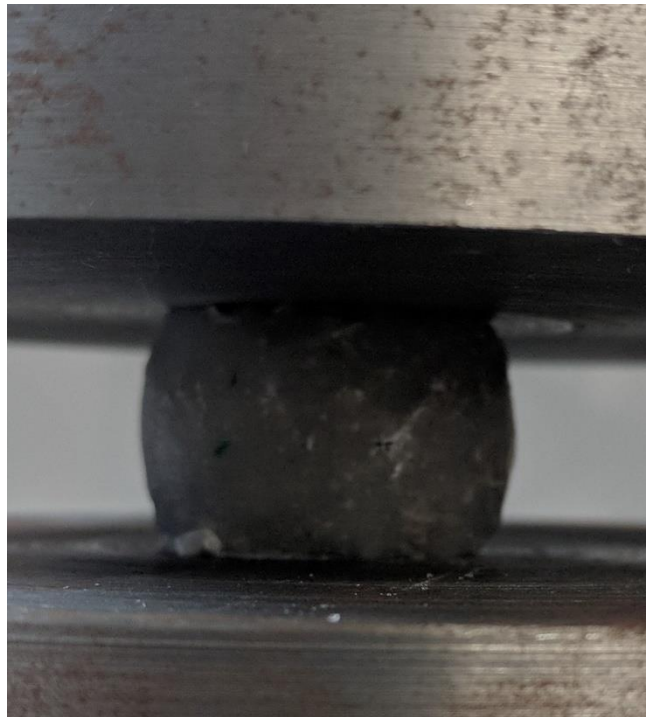
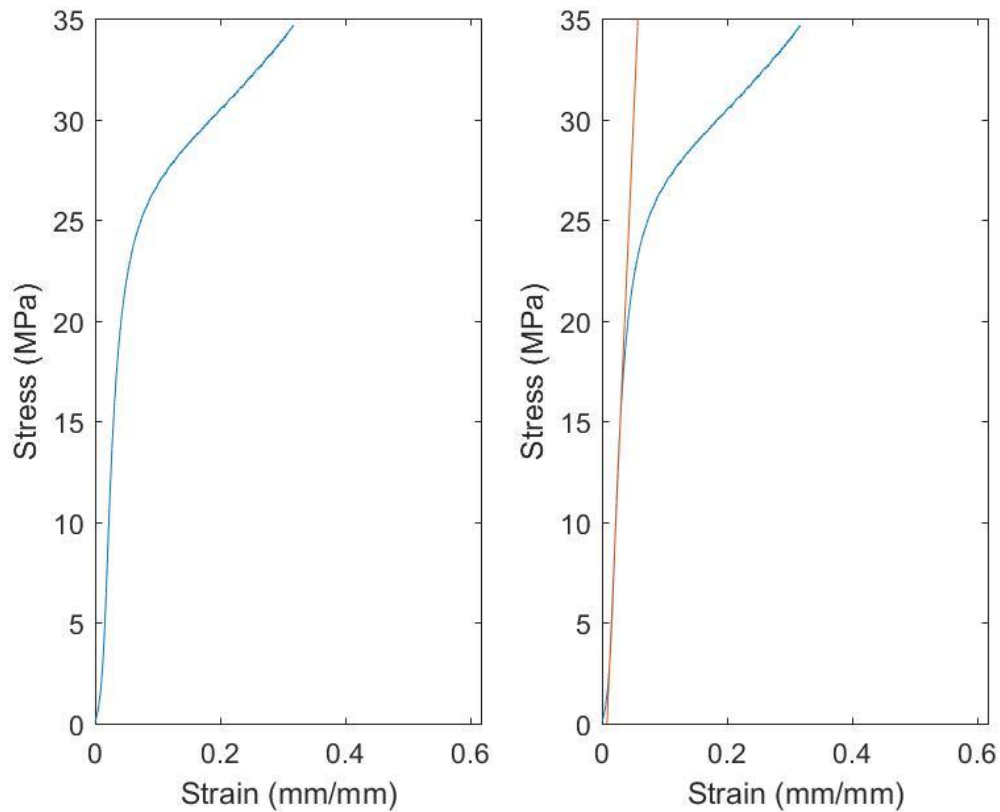


Figure 30. 50%HDPE/ FS Compression Sample with Stress Crack and Mushrooming

Like the flexural tests, force and displacement data was used and analyzed in MATLAB to generate a stress-strain curve, and to determine the Modulus of Elasticity, Ultimate Compressive Stress (UCS), and 0.2% Offset Yield Stress. A representative curve is shown in Figure 31 of a 50% HDPE/FS sample. In the graph, it is apparent that the stress would continue to increase steadily until the sample became a flat disk if the failure criteria previously discussed was not defined. The mushrooming and surface cracks or ruptures typically occurred about 4-5-minutes after starting the tests. Samples with more plastic tended to last longer as they could deform more before showing surface defects.



**Figure 31. (Left) Stress Strain Curve for 50% HDPE/FS Compression Specimen
(Right) Stress-Strain with Modulus of Elasticity Fit Line**

The maximum load on the stress-strain curve is the UCS; however, the Yield Stress again is of more interest and relevance. Pure HDPE had a compressive yield strength range of 19.82 to 28.67 MPa, giving an average of 22.89 ± 3.62 . The radiograph inspection showed some air bubbles in the compression samples. The more significantly damaged specimens were not included in the testing, but samples still had some air bubbles affected the resulting strength. The accepted range of compressive strengths for concrete is 20-40 MPa, so HDPE is on the lower end of that range. The strength of concrete was not expected to be exceeded with the thermoplastic concrete, in fact it is indeed lower, but using it as a comparison useful. Also, the structures intended to be built with the thermoplastic concrete are not meant to need to support a significant amount of weight, being only one story. On most other extraplanetary bodies being considered for exploration, gravity is much less than on earth, which means that habitat structures do not need as much strength as they would on earth.

Mixing HDPE with CS produced lower UCS, as expected. The yield stress remained similar to pure HDPE, with a slight increase, except for the 20% mixture which was significantly lower. As a first thought, it is surprising that the CS increased the strength in compression. However, after more consideration the larger particle size would mean more collisions internally, and since sand does not deform, the yield stress would be higher. The sand particles compressed steadily in the linear region before the HDPE yielded. FS decreased the yield stress, but results were again more consistent with smaller standard deviations. The effects of the smaller particle size are perhaps more apparent in the compressive tests based on the strength reductions. Tests also took slightly longer – about 30 seconds on average – to complete with the FS mixtures. The fine particles

would compress together more and would take longer to be pushed out of the surface of the sample. Figure 32 shows the graph of compressive Yield Strength vs. Plastic Percentage.

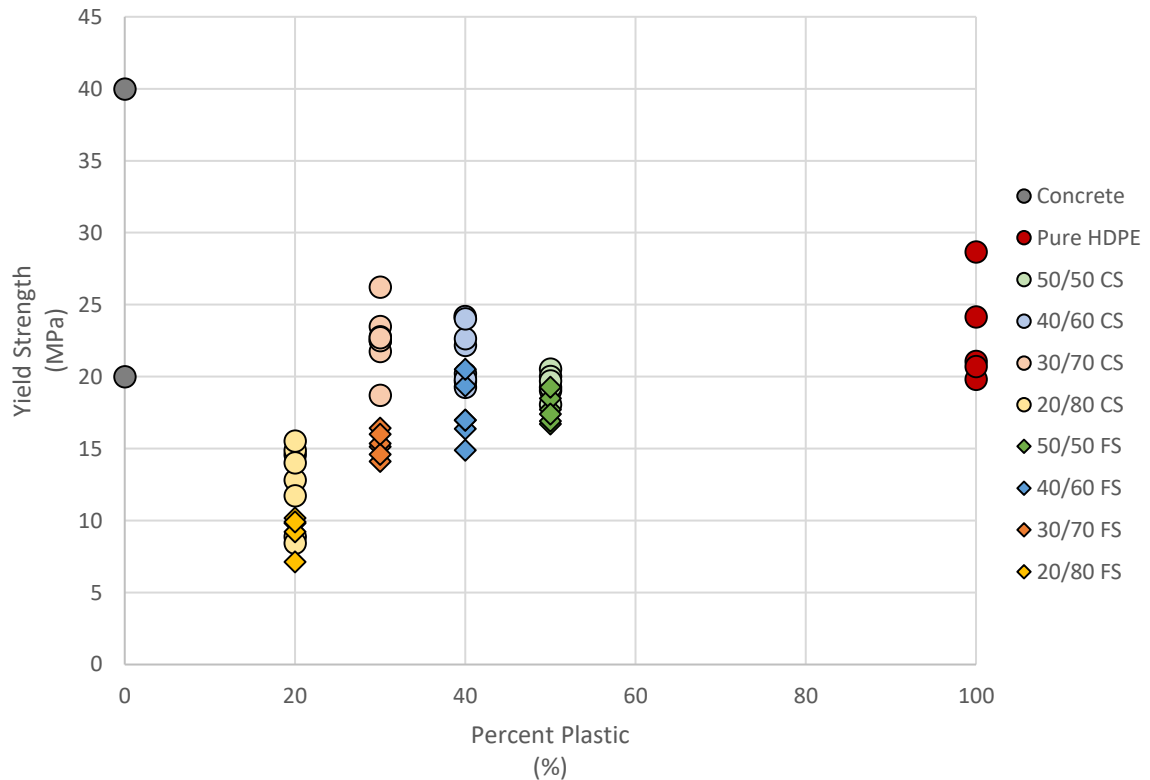


Figure 32. Compressive Yield Strength vs. Plastic Percentage

Yield stress is lower between the CS and FS samples across all mixtures, but the 30% HDPE/FS has the largest difference, while being less variable overall. The yield stresses in the 30% HDPE/FS have a lower standard deviation much like the flexural tests but are lower. It appears that what may have been a benefit for flexural strength may be a detriment in compressive strength, an even distribution and mixing of the HDPE and FS aggregate would maintain overall strength better and hold together, but the sand particles could fill in between each other easier with more deformation, lowering yield stress.

Also, in compression the material is compacted together and there could have been micro-channels or pockets of air since the plastic percentage was still relatively low. These air pockets would affect the yield strength more in compression than flex since the HDPE would simply be crushed to fill the voids. Even with this decrease compared to CS, the consistency of 30% HDPE/FS makes planning and building design simpler and more reliable. The standard deviation the FS mixture is ± 0.86 MPa, compared to the CS mixture of ± 2.06 MPa.

The Modulus of Elasticity calculations produced some surprising results. For CS mixtures, the results are opposite of flexural testing, where Yield Strength decreased with increasing Modulus of Flexure. In compression, the average Yield Strength increased, except for the 20% mixture, while Modulus of Elasticity decreased in a linear fashion. The most likely explanation is that there were more air bubbles in the CS mixtures. More evidence supporting this conclusion is given by the relatively large standard deviation in Modulus of Elasticity. The 30% mixture, for example, has a standard deviation of about half the average. This meant the particles were displaced steadily to fill in air gaps but was still able to resist stress until the walls of the cylinder gave out. The FS Modulus of Elasticity makes more sense. The average Yield Strength of 40% and 50% HDPE/FS samples was relatively similar, and so was the Modulus of Elasticity for the same mixtures. The 30% Modulus increased, whereas the Yield Strength decreased, and the 20% HDPE/FS values both dropped, showing it could not resist stress well. Figure 33 shows a plot of the average Modulus of Elasticity Values with standard deviations, and Table 2 shows the average values of UTS, Yield Strength, and Modulus of Elasticity for the compression tests.

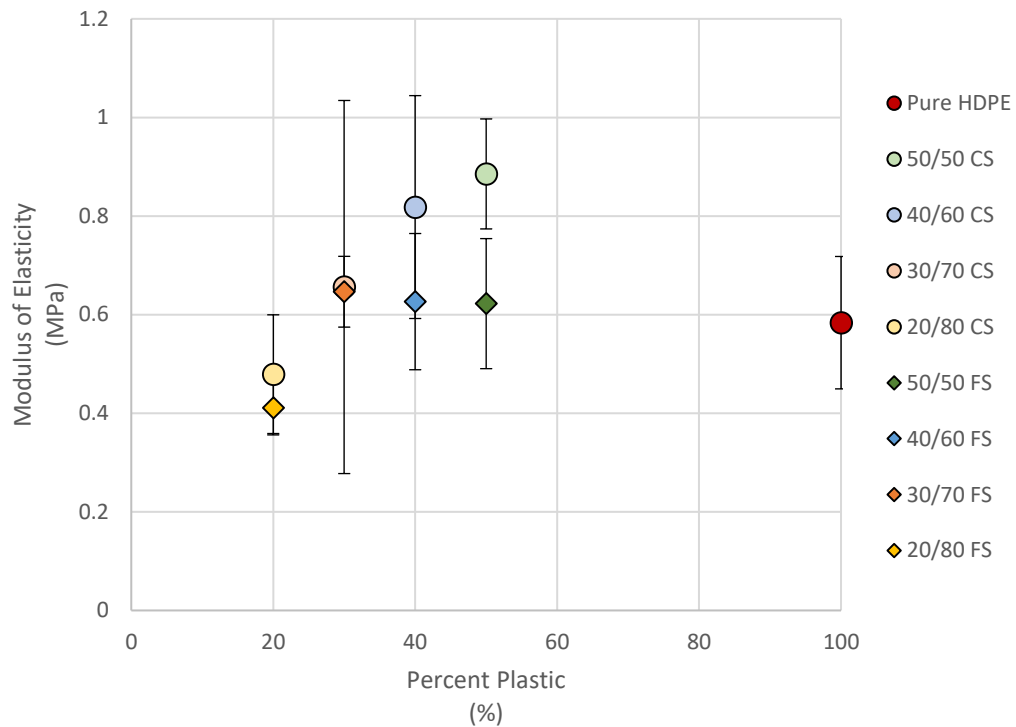


Figure 33. Modulus of Elasticity vs Percent Plastic for Compression Samples

Table 2. Average Compressive Strength Values of Pure HDPE, CS, & FS Mixtures

Mixture	UCS (MPa)	Yield Stress (MPa)	Modulus of Elasticity (GPa)
100	46.57 ± 8.72	22.89 ± 3.62	0.58 ± 0.13
50% HDPE/CS	32.18 ± 1.39	19.45 ± 0.86	0.87 ± 0.11
40% HDPE/CS	33.69 ± 4.13	21.5 ± 2.01	0.82 ± 0.23
30% HDPE/CS	29.33 ± 5.49	22.59 ± 2.06	0.66 ± 0.38
20% HDPE/CS	14.82 ± 4	12.62 ± 2.71	0.48 ± 0.12
50% HDPE/FS	32.09 ± 3.2	17.75 ± 0.98	0.62 ± 0.13
40% HDPE/FS	26.96 ± 1.48	17.52 ± 2.06	0.63 ± 0.14
30% HDPE/FS	24.85 ± 0.72	15.27 ± 0.86	0.65 ± 0.07
20% HDPE/FS	12.19 ± 3.12	9.26 ± 1.24	0.41 ± 0.05

From compressive strength testing, a 30% mixture would be sufficient to be used in the 3DPH Challenge. The CS mixture had an average Yield Strength above the lower end of concrete, however, the standard deviation was high. The FS mixture was desired

despite being lower by about 7 MPa on average. The reliability of the tested samples was more important to building design than a higher strength. Since a 30% HDPE/FS mixture was desired for the flexural strength as well, a 30% HDPE/FS aggregate mixture was used during print quality tests, discussed in a later section. After determining good print quality setting, samples would be cut from successful blocks and used for flexural and compression testing to compare printed to molded strength.

4.4 3D Printed Habitat Challenge Printer

During molded material testing and analysis, the SDSU team for the 3DPH Challenge designed and built a large-scale 3D printer capable of printing the HDPE/sand composite material. The build was completed at the SDSU Mechanical Engineering shop. The building process started with the X rails and progressed steadily from there. Using a 3D printed jig to fit the angles correctly in the U-channel, shown Figure 34, the three parts were welded together. After welding, the tower legs could be assembled and fit to the track, with part of the process shown in Figure 35. The gantry, shown in Figure 36, stands about ten feet tall from the shop floor and is four feet wide at the base.



Figure 34. X-Axis Rail Jig Assembly

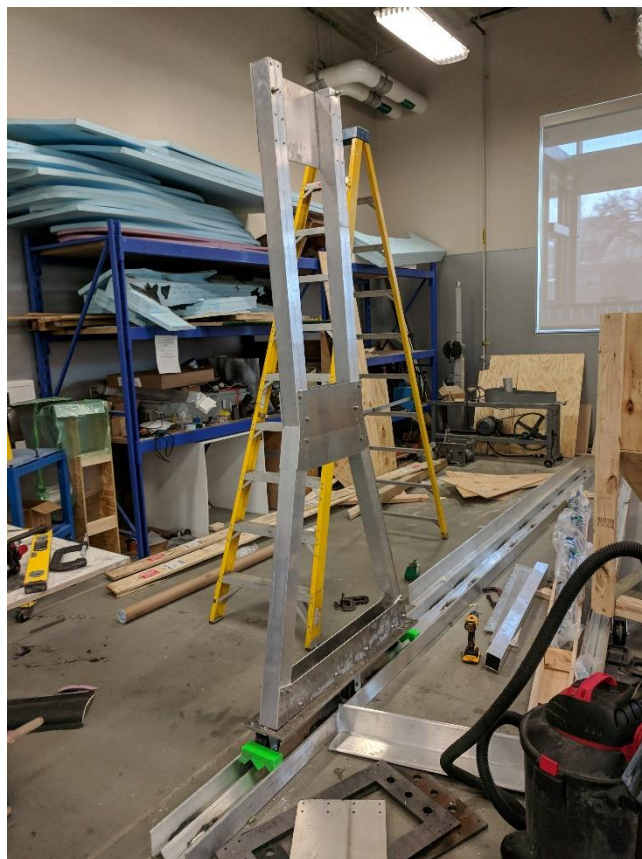


Figure 35. Tower Build in Progress



Figure 36. Completed Printer

The X-axis motion system worked extremely well, and the V casters keep the towers aligned without issue. Another benefit of the casters is that they can be rolled off the end and rolled around the shop for easy transportation. This will be extremely useful in the future as further research plans with the system may require new structure designs. If the V casters can be rolled off and out of the way, other types of printers can very easily be set up and tested without needing a lot of down time. A closer view of the V casters and track is shown in Figure 37, and one of the X-Axis motors and rack system is shown in Figure 38.



Figure 37. V Caster Track

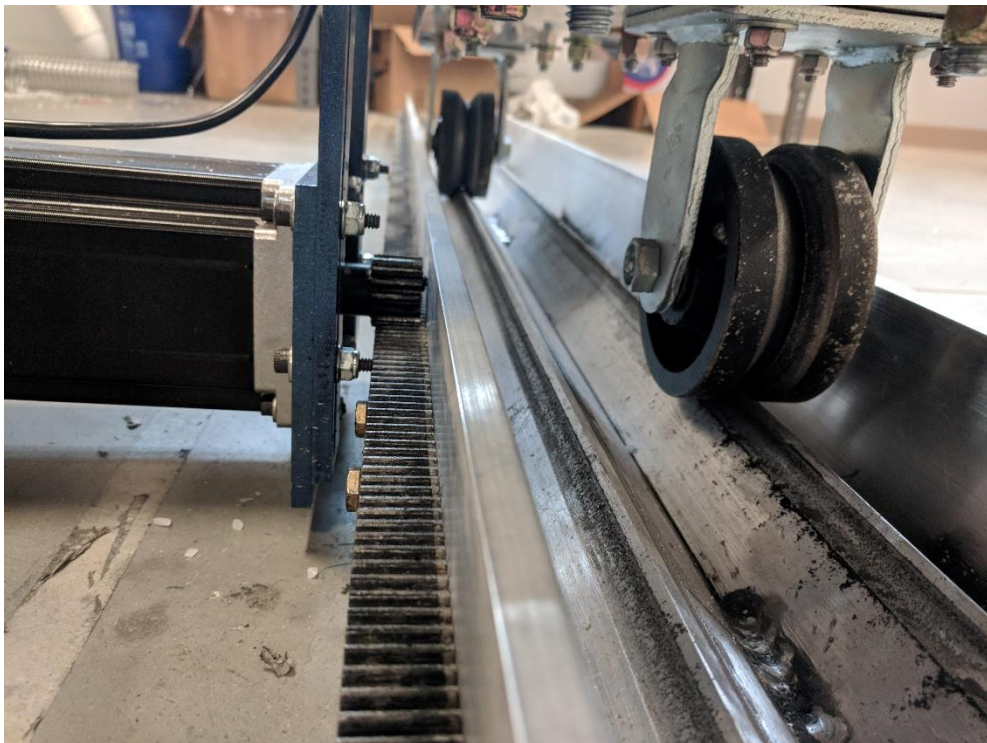


Figure 38. X-Axis Motor and Rack

After proper alignment the Y-axis runs very well. The beams also support the weight of the print head and more. Extra weights were added to the print head structure and a level was placed to one side with no visible deflection or slope change. Figure 39 shows an end view of the Y-axis. The two plates that make up the carts for the Y-Axis support the print head structure. The entire print head moves up and down through large holes in the plates, shown in Figure 40. The full print head will have more components added later for the 3DPH Challenge. These will make up an autonomous material handling system that will automatically transfer material to the print head and measure and mix the correct sand/HDPE ratio. However, for initial testing and printing this is not necessary. A full view of the print head is shown in Figure 41.

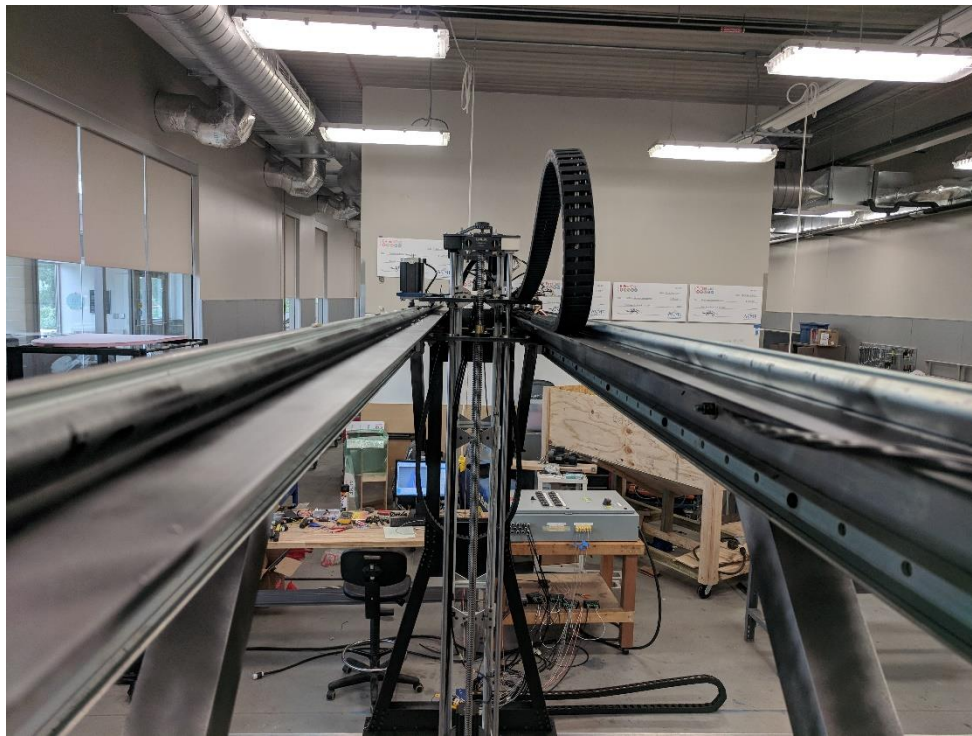


Figure 39. Y-Axis End View

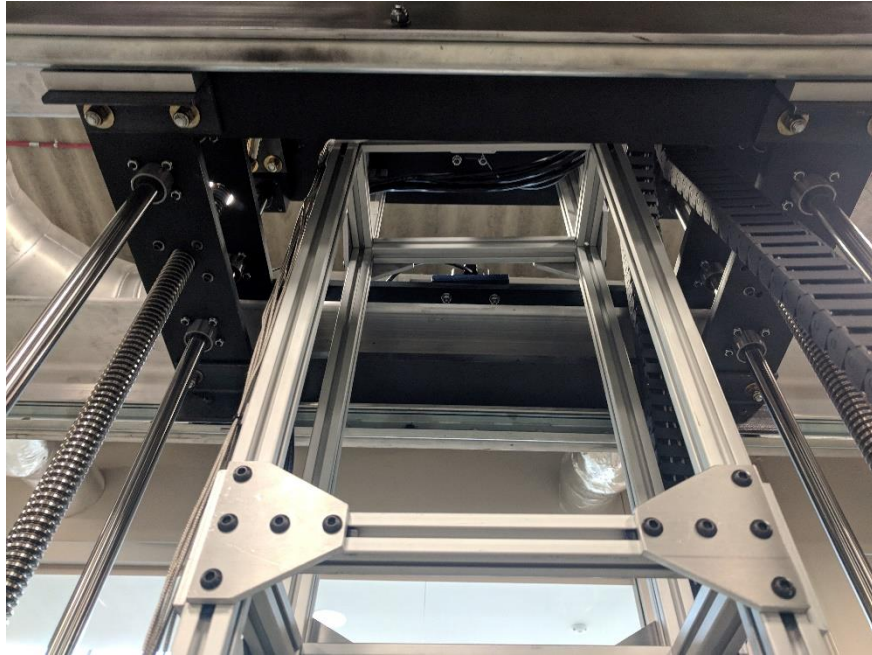


Figure 40. Y-Axis Print Head Opening



Figure 41. Full View of Print Head

The Z-Axis is built in to the print head and uses two lead screws with a single motor attached via a sprocket and chain system, shown in Figure 42. The three smaller gears are idler gears mounted to a bearing. These are used to reduce the slack in the chain and can be adjusted as needed. The flange and nut for the lead screw are mounted to the lower plate of the Y-Axis cart system so that the print head weight is supported in the strong direction of the bearing carts used for motion. The four linear rods are mounted around the plates with bushings mounted through the plate to provide extra reinforcement for the moment of the print head. Figure 43 shows a view of one side of the Y-axis cart where the lead screw mounts, and two of the linear rods pass through the bushings.

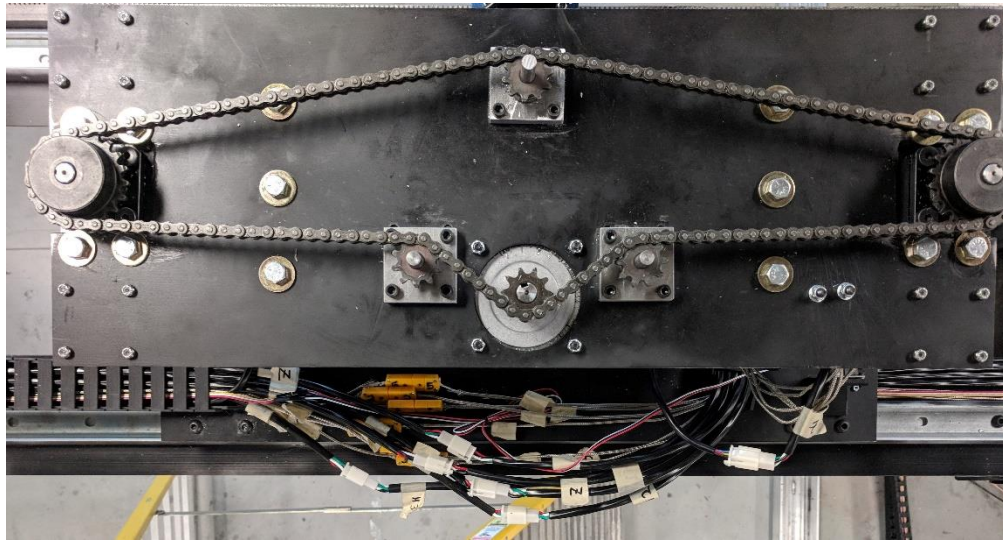


Figure 42. Z-Axis Motion System

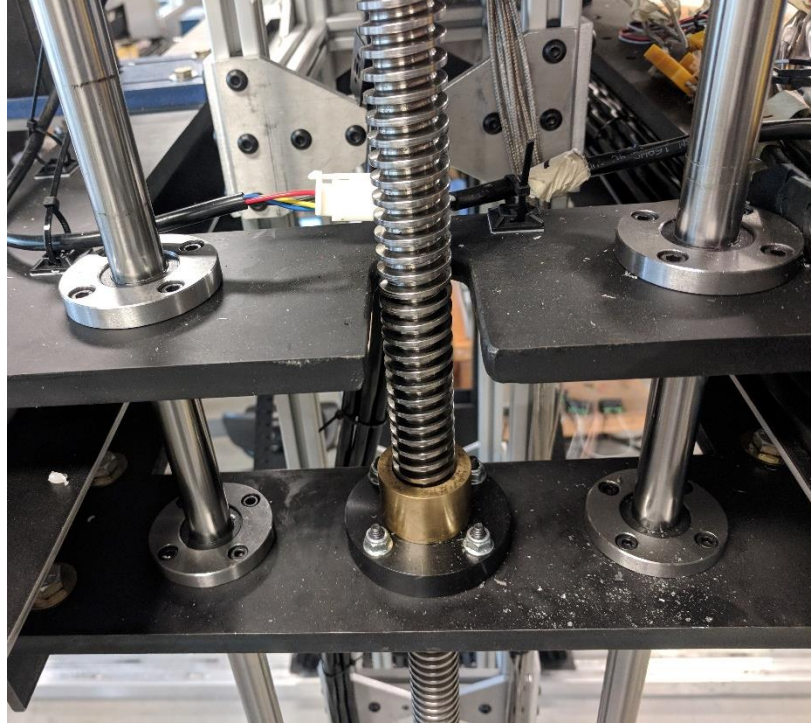


Figure 43. Lead Screw and Linear Rod Mounting

The last part of the printer is the extrusion system. The extrusion system is nearly identical to the original test printer, with some changes. Lessons learned from the small test printer showed that the extruder motor needed to have much more torque. The motor itself is stronger than the original, and there is also a 1:4 gear ratio to further increase torque. The motor is connected to the auger shaft by a gear chain system. The block and thrust bearing used to counteract the back pressure works as designed and limits the axial motion to a few millimeters. The eight heater bands were more than needed to heat the material and two of them were disconnected. Figure 44 shows the extruder motor system and Figure 45 shows the heater band and thermocouple setup.

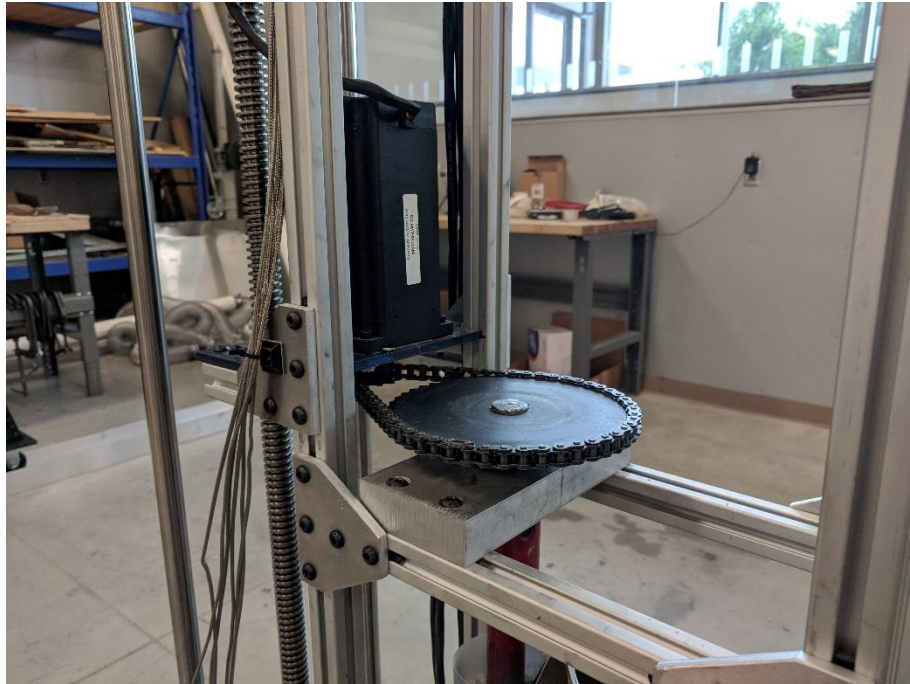


Figure 44. Extruder Motor System

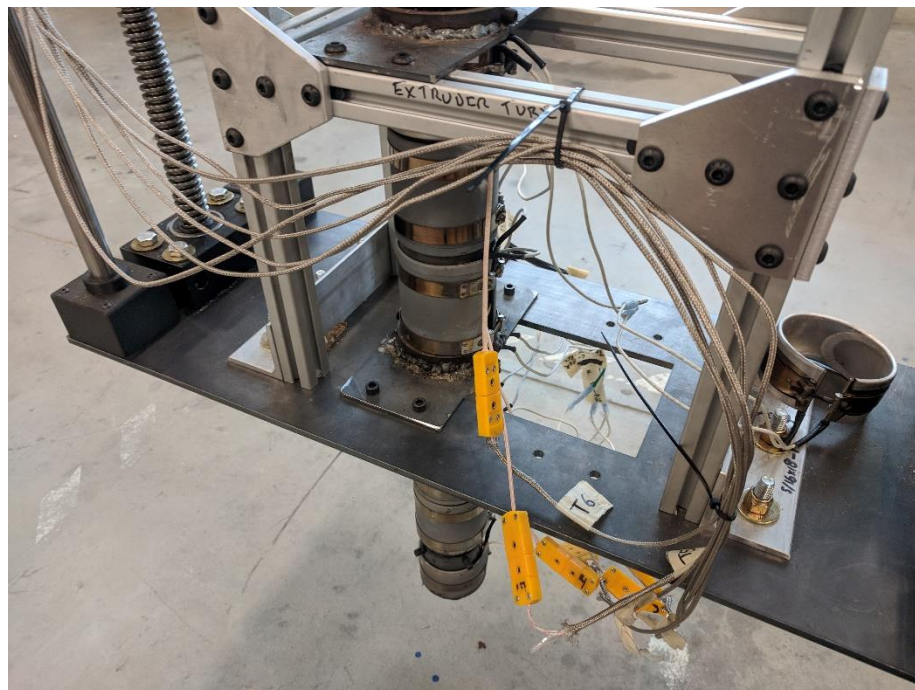


Figure 45. Extruder Heater Bands and Thermocouples

Extensive testing was done to ensure accurate motion of the system. X, Y, and Z motion. This was tested by sending the printer in the specified direction by a given distance and the change was measured. The printer was accurate to less than 0.01% in all directions, which is more than sufficient for the size of the printer. Extrusion calibration tests were done to match extrusion rate with printing speed to find good settings for early stages of printing.

4.5 Qualitative Print Tests

Printing quality tests were performed using the 3DPH Challenge Printer. Based on molded material testing, a 30% mixture using FS as the aggregate was used. For each sample, print speed, and extruder feed rate and steps/mm were adjusted on print-by-print basis. Print quality was determined by visual inspection, with common failure methods being line tearing and under extrusion. Figure 46 shows a failed print with evidence of tearing and under extrusion. Another failure is over extrusion, which affects layer height and line width. Too much material means the line width will be too wide and as the nozzle prints next to a previous pass, the material will be printed on top of the line next to it, which should only happen at a layer change. This affects layer height and can cause issue in the print. Figure 47 shows a sample with over extrusion, with uneven line width and overlap.



Figure 46. Final Results of First Test Print



Figure 47. Second Test Print Line Overlap

After five test prints, an acceptable print quality was achieved, with a minor over extrusion. The layer heights were slightly higher, resulting in material being pushed to the outside of the print, distorting the outside dimensions. Figure 48 shows print five in progress. A sixth print used a faster print speed to distribute the material and produced a good quality print. Figure 49 shows the sixth print in progress. The final print produced a dimensionally accurate sample with excellent layer adhesion.



Figure 48. Print Five in Progress



Figure 49. Test Print Six in Process

4.6 Printed Sample Strength Testing

After performing print quality tests, flexural and compressive test specimens were cut from rectangular blocks. The samples were cut because of the large layer size, which would affect the true cross-sectional area of any of the parts tested. The edges of the printed blocks had significant indents from layer boundaries and accurate calculations were desired, requiring samples to be cut and faced from the printed block.

From a qualitative viewpoint, the printed sample looks nearly identical to molded samples, however, the printed sample appears to be mixed better, as mixing occurred in the extruder because of the auger, while the HDPE was melted. This ended up producing a much better particle distribution than could be achieved by ‘dry’ mixing in the molded samples. A comparison of a printed flexural block and a 30% HDPE/FS molded flexure block is shown in Figure 50. Note the left edge of the molded sample on the right. There

are a few sections that look as if there are no sand particles and is pure HDPE. The molded sample also looks as if aggregate is not evenly distributed and there are spots where is grouped tightly with minimal HDPE filling gaps. Looking at the printed sample shows a much different result, with a significantly more even distribution with no gaps in sand distribution and effective HDPE distribution between the sand particles, while still looking to be made with the same amount of sand based on visual inspection. It is also apparent that the printing process leaves no indication of layers, other than the outside edges.



Figure 50. Comparison of Printed (left) and Molded (right) Flex Samples of 30% HDPE/FS

Flexural testing was using the same method as the molded samples, with a change to the span because of a slightly larger beam size. The material is highly abrasive and

after cutting needed facing. If samples were faced to the same approximate size as the molded samples there would have been severe damage to the tools. To save tooling, the beams were just faced to a larger size and the span was doubled to accommodate the additional material and potential increased load capacity. A printed beam during testing is shown in Figure 51 with the larger span.



Figure 51. Printed Flexural Sample in Test Fixture

Compression testing was also performed on the printed sample, using a rectangular prism in this case. The ASTM standard for compression allows for square cross-sectional area samples and allows for the samples to be cut from larger blocks of material. The compression samples were cut to have a 25mm square area, and to be at least 50mm long to get a proper slenderness ratio for the test. Figure 52 shows the compression samples. Testing was completed using the same fixture and load rate as the molded samples. The failure criteria were the same as molded samples as well and

mushrooming was a little more obvious with a square sample. Figure 53 shows a specimen after failing in the test fixture.



Figure 52. Printed Compression Samples



Figure 53. Printed Compression Sample After Failure

Flexural test results show a slight increase in the Yield Strength from a molded sample, moving from an average of 14.02 ± 1.59 MPa to 16.55 ± 0.32 MPa. The Modulus of Flexure also increased significantly from 0.63 ± 0.09 , to 1.97 ± 0.06 GPa, which is

also a major increase over pure HDPE. Table 3 shows the flexural strengths of the full set of tested samples. Compression samples show similar improvements, increasing the compressive yield strength of 30% HDPE/FS mixture from 15.27 ± 0.86 to $21.61 \text{ MPa} \pm 0.04 \text{ MPa}$. The Modulus of Elasticity also increased from $0.65 \pm 0.07 \text{ GPa}$ to $1.62 \pm 0.88 \text{ GPa}$. Table 4 shows the compressive strengths of all tested samples for easy comparison as well.

Table 3. Flexural Strength Values for All Tested Samples

Mixture	Mod Rupture (MPa)	Yield Stress (MPa)	Modulus of Flexure (GPa)
100	43.02 ± 4.11	20.24 ± 1.16	0.49 ± 0.03
50% HDPE/CS	24.99 ± 4.37	16.57 ± 1.45	0.62 ± 0.11
40% HDPE/CS	21.46 ± 2.07	16.96 ± 1.3	0.67 ± 0.14
30% HDPE/CS	14.89 ± 2.01	13.73 ± 1.67	0.63 ± 0.15
20% HDPE/CS	12.47 ± 1.77	12.19 ± 1.66	0.68 ± 0.06
50% HDPE/FS	22.8 ± 3.11	13.56 ± 1.64	0.5 ± 0.03
40% HDPE/FS	18.35 ± 1.15	12.18 ± 0.63	0.55 ± 0.07
30% HDPE/FS	16.68 ± 1.02	14.03 ± 1.59	0.63 ± 0.09
20% HDPE/FS	8.57 ± 2.97	5.44 ± 3.82	0.44 ± 0.12
30% HDPE/FS Printed	19.29 ± 0.63	16.55 ± 0.32	1.97 ± 0.06

Table 4. Compressive Strength Values for All Tested Samples

Mixture	UTS (MPa)	Yield Stress (MPa)	Modulus of Elasticity (GPa)
100	46.57 ± 8.72	22.89 ± 3.62	0.58 ± 0.13
50% HDPE/CS	32.18 ± 1.39	19.45 ± 0.86	0.87 ± 0.11
40% HDPE/CS	33.69 ± 4.13	21.5 ± 2.01	0.82 ± 0.23
30% HDPE/CS	29.33 ± 5.49	22.59 ± 2.06	0.66 ± 0.38
20% HDPE/CS	14.82 ± 4	12.62 ± 2.71	0.48 ± 0.12
50% HDPE/FS	32.09 ± 3.2	17.75 ± 0.98	0.62 ± 0.13
40% HDPE/FS	26.96 ± 1.48	17.52 ± 2.06	0.63 ± 0.14
30% HDPE/FS	24.85 ± 0.72	15.27 ± 0.86	0.65 ± 0.07
20% HDPE/FS	12.19 ± 3.12	9.26 ± 1.24	0.41 ± 0.05
30% HDPE/FS Printed	24.00 ± 1.62	21.61 ± 0.04	0.88 ± 0.26

The increase in strength overall is impressive, and somewhat unexpected. The Modulus of Flexure is also significantly higher than pure HDPE. The strength testing was meant to be a confirmation of material composition aside from a visual inspection, but the change was so significant that more investigation was needed.

Another way to verify material composition is to compare material densities. The density of molded samples was calculated before testing for use in calculations for printing and material mixing, and the density of the printed samples was also measured using the flexure samples. Table 5 shows the average sample densities from molded and printing tests.

Table 5. Densities of All Mixture Types

Mixture	Density (kg/m ³)
100	915.97 ± 9.8
50% HDPE/CS	1326.23 ± 25.89
40% HDPE/CS	1433.49 ± 19.45
30% HDPE/CS	1752.81 ± 53.84
20% HDPE/CS	1739.76 ± 34.65
50% HDPE/FS	1290.36 ± 19.12
40% HDPE/FS	1423.93 ± 48.53
30% HDPE/FS	1586.9 ± 17.03
20% HDPE/FS	1612.06 ± 18.74
30% HDPE/FS Printed	1658.65 ± 6.36

Comparing the densities, a much larger deviation in the molded samples compared to the printed samples is obvious. There is a huge difference in the densities of the 20% and 30% HDPE/FS and CS samples. The 20% and 30% HDPE/CS samples have almost an identical density. Looking at the flexural tests this makes sense as the test results are similar, differing by less than 2 MPa. The FS samples appear to follow a trend that seems reasonable given the difference in plastic content. However, even here the 20% and 30% mixtures do not differ by much compared to other ratio jumps. Overall, the deviations for the FS samples is much less than the CS samples, which most likely has a lot to do with particle sizes. If there is an uneven distribution of the large particles across samples of a given mixture ratio, the densities will be fall across a broader range. Again, a smaller particle size leads to more consistent results. Finally, the printed sample shows a higher density than even the 20% HDPE/FS mixture. It also has a smaller deviation than any other mixture, including pure HDPE.

One final comparison was made to verify the composition of printed material. A radiograph inspection was done using the 30% HDPE/FS printed sample, and a 20% and 30% HDPE/FS molded sample. The radiograph image is shown in Figure 54, and Figure 55 shows a color corrected radiograph that shows plastic and sand distribution more clearly. From these two figures it is obvious the printed sample is denser than either the 20% or 30% molded samples. There is also evidence of small air pockets scattered in the molded samples, as well as areas of more concentrated sand.

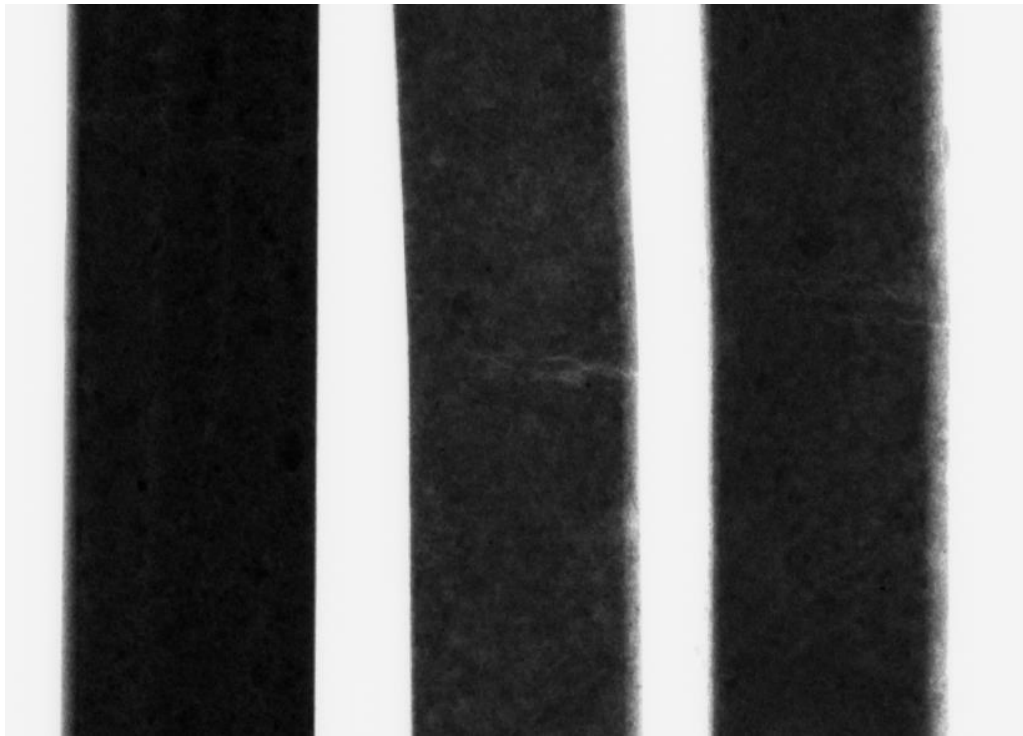


Figure 54. Radiograph of 30% HDPE/FS Printed Sample (left), 20% Molded Sample (middle), and 30% Molded Samples (right)

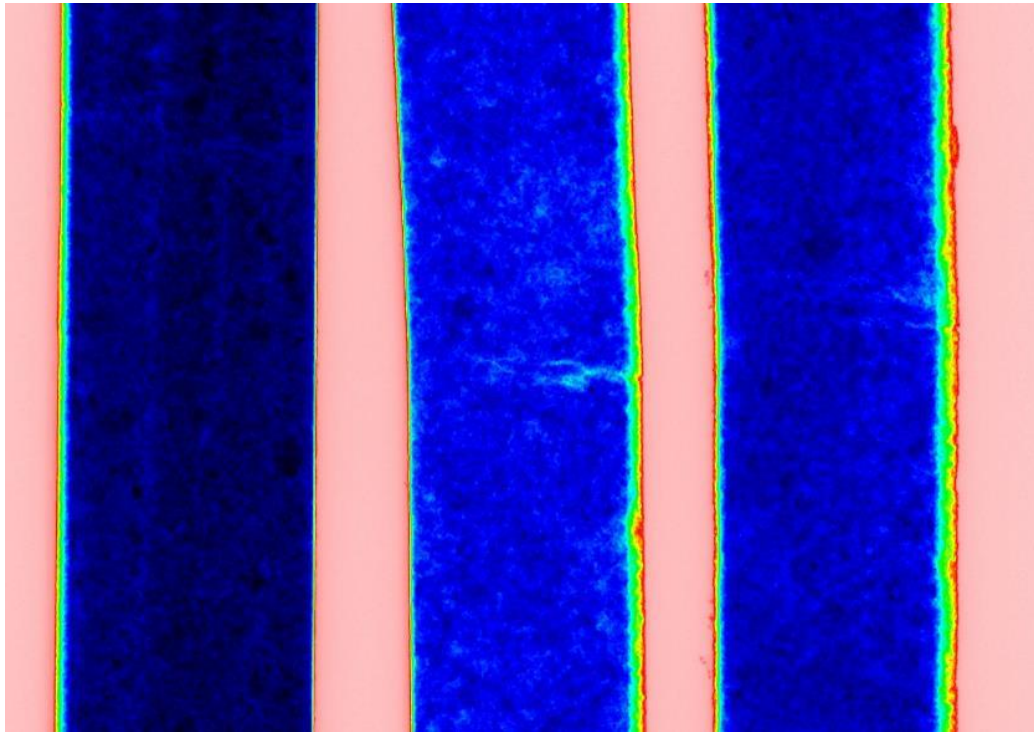


Figure 55. Color Corrected Radiograph of 30% HDPE/FS Printed Sample (left), 20% Molded Sample (middle), and 30% Molded Samples (right)

Not only does it appear that the printed sample is stronger, it also has a higher density than a 30% HDPE/FS mixture. There are multiple implications because of this which would require further research in to the mixing, melting, and forming processes. First, the printed sample has a higher density, meaning there is more sand per volume than the molded samples have. There may also be fewer micro air pockets trapped in the material as the melted mixture is compressed in the extruder. It also has a higher strength than the same mixture of molded samples. These two results together could mean a mixture using even less plastic than the 30% mixture being considered, could produce the same results as molded 30% plastic. This has the benefit of using less plastic for the 3DPH competition, and for the potential use on extraterrestrial bodies where importing plastic will be expensive, if not impossible.

Another implication is that simply heating and mixing the materials before forming will significantly benefit material properties. In the 3D printer developed for the challenge this is already done to some extent in the extruder. However, a premixing system may also be a good option to have for the team but would require multiple changes to the design and control system concept. For other applications though, thorough mixing would be a major benefit. Since another potential use for the material is to build small structures on Earth, a heated mixing system would produce more reliable parts or structures.

CHAPTER 5: CONCLUSIONS

The increasing focus on 3D printing and AM techniques in the construction industry is opening the door for innovative technologies and materials. The potential is already being demonstrated in labs across the world for using AM techniques to create construction scale prints.

The space industry has also been looking in to using 3D printing to create more intricate parts at a lower cost, with successful tests done by SpaceX and NASA. NASA has also shown major interest in using construction scale AM to create habitats for manned missions on extraplanetary bodies. They created the 3D Printed Habitat Centennial Challenge to start boosting interest and research in this field by offering prize money to competitors across the globe. The centennial challenge was a major motivator for research in a thermoplastic concrete that could be 3D printed, as well as the potential use for removing waste plastic from the environment here on Earth by using the material for small scale structures such as sidewalks, parking lots, low traffic roads and landscaping architecture.

Initial research on materials was promising, starting with using a sulfur concrete; however, research was soon stopped along this path after running in to difficulties and hazards working with the material. Further details provided by NASA on the 3DPH Challenge revealed a materials list that NASA is interested in, primarily using thermoplastics as a binding agent. PET and HDPE were considered, with HDPE being the top choice, both by NASA, and for research because of its lower melting temperature and relatively easy workability. PET becomes very brittle after melting which makes it

less suitable to print with. Siliceous sedimentary rock, or simply sand, aggregate was also chosen for its easy sourcing and low cost, despite only being in the middle rankings for the competition. The sand only acts as a filler material in the specimens and does not really react with the plastic. In this case the sand is meant to represent a general aggregate material rather than a critical component to the mixture.

Molded sample tests showed varying strengths, with a trend to decrease in strength as the plastic content decreased. This result was expected, however, despite this, the flexural strength of the thermoplastic concrete is better than standard concrete. The compressive strength is comparable to standard concrete but showing much more yielding (less stiffness) overall. A 30% plastic mixture was selected as a sufficient ratio for its good strength properties and low plastic content. Molded test results also indicated that FS produces more consistent results, even though it has slightly lower strengths. The lower strength has multiple potential causes. The first being a tighter packing of the sand particles, preventing HDPE from properly filling gaps. The lack of mixing during the melt process also makes this a reasonable problem. The small particles also likely compress between each other when under a compressive stress, rather than colliding and resisting stress like larger particles would. More research and potential simulation work would need to be done to confirm this theory. The optimum mixture was decided to be the 30% wt. FS mixture, with a flexural yield stress of 14.03 ± 1.59 MPa, and a compressive yield stress of 15.27 ± 0.86 MPa. Despite the lower compressive yield stress compared to standard concrete, a 30% wt. HDPE/70% wt. FS mixture would be used for printing.

A printer for the 3DPH Challenge was completed designed and prototyped for printing test samples. Full mobility via NEMA 34 motors and systems of gear racks, sprocket-and-chain, and lead screws allow the printer to move and print in a 3000x4500x2400 mm print area. Early print tests required iterative testing because of the unique nature of the extrusion system. Proper settings were eventually identified, and a print speed of 10 mm/s was reached, which will be slow for the large area the habitat requires, but for initial testing purposes is perfect. Printed samples were made to be tested in flex and compression.

The printed samples made with a 30% wt. HDPE/ FS mixture exceeded expectations. The samples were cut from a larger printed block to reduce errors from the layer effects on the edges of the part. The layer effects only existed along the outer edges however, as the middle of the part showed no indication that the part was printed. Layer bonding was so good that there were effectively no layers, and the samples were one coherent part. Flexural and compressive yield strength improved to 16.55 ± 0.32 MPa and 21.61 ± 0.04 MPa, respectively. The increase in strength and lower deviation was surprising and has largely been attributed to the mixing and heating process. Molded samples were mixed dry and then heated in an oven, whereas the printed sample had material dumped in to the extruder unmixed. The materials were mixed by the auger and evenly distributed. Visually, the printed part looked homogenous throughout, with no obvious areas where mixing did not occur. This result also implies that proper mixing and heating of a lower plastic mixture could improve the strength enough to make it a viable mixture as well, further reducing the plastic content needed for a trip to another planet.

A material comprised of 30% wt. HDPE, and 70% wt. has been tested and selected to be used for the 3D Printed Habitat Challenge created by NASA to develop new technologies to aid in the manned exploration of other planetary bodies in the solar system. Flexural and compressive strength testing show the material has sufficient strength properties to be used, which are further increased by the printing process, because of the mixing and heating done in the extruder. A large 3D printer capable of printing and competing in the 3DPH challenge was also designed and built and the material is easily extruded by the system.

Further research in to material properties would include more detailed research in to the effects of particle size on the mixture, as well as proper mixing times and processes. More research is also needed if this material were to be used on Earth for small construction projects. There is no known data on the environmental impact this material may have to any ecosystem. More experiments could also be completed using different aggregate types to learn how they affect properties, if at all. The print process will also need more refinement before being fully ready to compete in the 3DPH challenge but is working well for early printing tests.

REFERENCES

- [1] Malik, T., 2018, "Success! SpaceX Launches Falcon Heavy Rocket on Historic Maiden Voyage."
- [2] "Around the Moon with NASA's First Launch of SLS with Orion," <https://www.nasa.gov/feature/around-the-moon-with-nasa-s-first-launch-of-sls-with-orion>.
- [3] Musk, E., 2017, "Making Humans a Multi-Planetary Species," *New Space*, 5(2), pp. 46-61.
- [4] "NASA Tests 3-D Printed Rocket Part to Reduce Future SLS Engine Costs," <https://www.nasa.gov/exploration/systems/sls/nasa-tests-3-d-printed-rocket-part-to-reduce-future-sls-engine-costs>.
- [5] "SpaceX Launches 3D-Printed Part to Space, Creates Printed Engine Chamber," <http://www.spacex.com/news/2014/07/31/spacex-launches-3d-printed-part-space-creates-printed-engine-chamber-crewed>.
- [6] "NASA Opens \$2 Million Third Phase of 3D-Printed Habitat Competition," https://www.nasa.gov/directorates/spacetech/centennial_challenges/3DPHab/nasa-opens-2M-third-phase-of-3d-printed-habitat-competition.
- [7] Khoshnevis, B., and Dutton, R., 1998, "Innovative Rapid Prototyping Process Makes Large Sized, Smooth Surfaced Complex Shapes in a Wide Variety of Materials," *Materials Technology*, 13(2), pp. 53-56.
- [8] Khoshnevis, B., 2004, "Automated construction by contour crafting—related robotics and information technologies," *Automation in Construction*, 13(1), pp. 5-19.
- [9] Khoshnevis, B., Hwang, D., Yao, K. T., and Yeh, Z., 2006, "Mega-scale fabrication by Contour Crafting," *International Journal of Industrial and Systems Engineering*, 1(3).
- [10] Wan, L., Wendner, R., and Cusatis, G., 2016, "A novel material for in situ construction on Mars: experiments and numerical simulations," *Construction and Building Materials*, 120, pp. 222-231.
- [11] Khoshnevis, B., Yuan, X., Zahiri, B., Zhang, J., and Xia, B., 2016, "Construction by Contour Crafting using sulfur concrete with planetary applications," *Rapid Prototyping Journal*, 22(5), pp. 848-856.
- [12] Khoshnevis, B., Thangavelu, M., Yuan, X., and Zhang, J., 2013, "Advances in Contour Crafting Technology for Extraterrestrial Settlement Infrastructure Buildup," *AIAA SPACE 2013 Conference and Exposition*.
- [13] Letcher, T., Rankouhi, B., and Javadpour, S., 2015, "Experimental Study of Mechanical Properties of Additively Manufactured ABS Plastic as a Function of Layer Parameters," *Volume 2A: Advanced Manufacturing*.
- [14] Kazemian, A., Yuan, X., Cochran, E., and Khoshnevis, B., 2017, "Cementitious materials for construction-scale 3D printing: Laboratory testing of fresh printing mixture," *Construction and Building Materials*, 145, pp. 639-647.
- [15] Zareiyan, B., and Khoshnevis, B., 2017, "Interlayer adhesion and strength of structures in Contour Crafting - Effects of aggregate size, extrusion rate, and layer thickness," *Automation in Construction*, 81, pp. 112-121.
- [16] Gosselin, C., Duballet, R., Roux, P., Gaudillière, N., Dirrenberger, J., and Morel, P., 2016, "Large-scale 3D printing of ultra-high performance concrete – a new processing route for architects and builders," *Materials & Design*, 100, pp. 102-109.

- [17] Goulas, A., and Friel, R. J., 2016, "3D printing with moon dust," *Rapid Prototyping Journal*, 22(6), pp. 864-870.
- [18] Bedi, R., Chandra, R., and Singh, S. P., 2013, "Mechanical Properties of Polymer Concrete," *Journal of Composites*, 2013, pp. 1-12.
- [19] Jo, B.-W., Park, S.-K., and Park, J.-C., 2008, "Mechanical properties of polymer concrete made with recycled PET and recycled concrete aggregates," *Construction and Building Materials*, 22(12), pp. 2281-2291.
- [20] Mahdi, F., Abbas, H., and Khan, A. A., 2010, "Strength characteristics of polymer mortar and concrete using different compositions of resins derived from post-consumer PET bottles," *Construction and Building Materials*, 24(1), pp. 25-36.
- [21] 2008, "Concrete - Properties," https://www.engineeringtoolbox.com/concrete-properties-d_1223.html.
- [22] "Solidworks," Dassault Systemes.
- [23] "Repetier-Host," 3D Printing Software, <https://www.repetier.com>.
- [24] ASTM D695, 2010, "Standard Test Methods for Flexural Properties of Unreinforced and Reinforced Plastics and Electrical Insulating Materials," ASTM International, West Conshohocken, PA April 2010
- [25] ASTM C78, 2015, "Standard Test Method for Flexural Strength of Concrete (Using Simple Beam with Third-Point Loading)," ASTM International, West Conshohocken, PA January 2016
- [26] ASTM D695, 2010, "Standard Test Method for Compressive Properties of Rigid Plastics," ASTM International, West Conshohocken, PA April 2010